INFORMATION TO USERS

University of Alberta

Loading of Craniofacial Implants

by

Kristin Lee Miller   ©

A thesis submitted to the Faculty of Graduate Studies and Research in partial fulfillment
of the requirements for the degree of Master of Science

Department of Mechanical Engineering

Department of Biomedical Engineering

Edmonton, Alberta

Fall 2000

Canada

University of Alberta

Library Release Form

Name of Author: Kristin Lee Miller

Title of Thesis: Loading of Craniofacial Implants

Degree: Master of Science

Year this Degree Granted: 2000

Kristin Lee Miller
3305-40A Avenue
Edmonton, Alberta, Canada
T6T 1P1

Date: Oct. 2, 2000
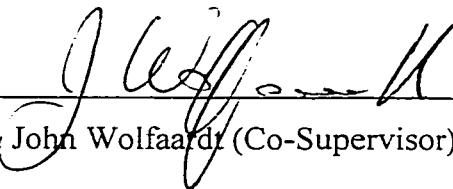
University of Alberta

Faculty of Graduate Studies and Research

The undersigned certify that they have read, and recommend to the Faculty of Graduate Studies and Research for acceptance, a thesis entitled **Loading of Craniofacial Implants** submitted by **Kristin Lee Miller** in partial fulfillment of the requirements for the degree of Master of Science.
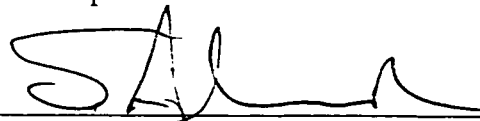
_____
Dr. M.G. Faulkner (Supervisor)

_____
Dr. John Wolfaardt (Co-Supervisor)

_____
Dr. A.W. Lipsett

_____
Dr. Scott Alexander

Date: Oct 2, 2000

Abstract

The purpose of this investigation was to develop an understanding of the type and magnitude of loads on craniofacial implants. To this end two loading situations for an auricular retention system were measured: the preload generated when attaching the framework to the abutments, and the functional loads generated during the attachment and removal of the prosthesis from the framework. The preload was measured both *in vitro* and *in vivo*, and compared to the clinically acceptable vertical misfit of 150μm. The functional loads generated were measured *in vivo* only.

The average preload generated by simply tightening the gold retention screw was −290N, which is comparable to the −300N expected when tightening the gold retention screw. No correlation was found between vertical misfit and the magnitude of misfit loads. The functional load distribution could indicate a difference in axial bending stiffnesses for different implant sites.

To my parents.

Acknowledgements

The process of writing a thesis is not accomplished without the help of others. I would like take this opportunity to thank the following people, without whom this study would not have been possible.

Dr. Faulkner and Dr. Wolfaardt for their patience and guidence with answering questions and pointing me in the right direction. The COMPRU team for their help during the *in vivo* tests and loaning me equipment. Dr. Don Raboud for his help with figuring things out and being a sounding board for my ideas, and for the other grad students in the lab for supplying a fun working environment.

Table of Contents

List of Tables

List of Figures

Chapter 1

Introduction

Loss of a portion of the face or neck due to disease or accident is a particularly traumatic

experience that causes both esthetic and functional disability. The use of silicone

prostheses that replace the missing portions are used to help rebuild the appearance and

lives of these individuals. The overall success of this treatment is dependent upon both

the construction of the prosthesis as well as the method with which it is attached. The

current methods used for prostheses construction produces prostheses that are practically

indistinguishable from real facial features. In the past, these prostheses were either glued

to the skin using medical adhesives or attached to glasses. Both methods left much to be

desired. The adhesives often caused adverse skin reactions, damaged the prosthesis, and

frequently displayed unpredictable performance. The use of glasses for prostheses

retention meant that the patient had to wear the glasses at all times and in addition, no

positive pressure could be placed on the prosthesis margins. The result was that the

margins of the prosthesis frequently displayed poor fit and the esthetic result was

diminished. In 1979 use of osseointegrated implants directly coupled to bone was first

introduced as a method of retaining facial prostheses. This allowed the prosthesis to attach to a stable anchoring point, which in turn improved the overall success of facial prostheses. Although 1979 was the first year that implants were used for retaining facial prostheses, osseointegration technology was not new as it had been in use in human trials since 1965.

1.1 Literature Review

1.1.1 History

In 1952, at the Laboratory for Vital microscopy, University of Lund, Sweden Professor Per-Ingvar Brånemark made an accidental discovery. During a study of the healing processes in bone, a titanium chamber containing an optical system was implanted into a rabbit's fibula. After the bone had healed the titanium chamber had become integrated into the bone and could not be removed. This type of bone-implant interface was later called *osseointegration* and is defined as "a direct structural and functional connection between ordered, living bone and the surface of a load-carrying implant" (Brånemark, et al., 1985, p.11).

This discovery lead to the use of titanium implants in human bone, in particular the use of implants in the mandible and maxilla (jaw bones) to act as the anchoring points for lost teeth. In 1965, the first edentulous (toothless) patient was treated with osseointegrated implants. The successful use of intraoral osseointegrated implants led to the use of extraoral (craniofacial) ossoeintegrated implants. In 1977, an osseointegrated implant was used as a retention system for a Bone Anchored Hearing Aid (BAHA®, Entific

Medical Systems, Gothenburg, Sweden), and then in 1979 they were introduced as anchoring points for facial prostheses.

1.1.2 Craniofacial Implants

Since their introduction in 1976, craniofacial osseo integrated implants, herein referred to as craniofacial implants, have been used successfully as a retention method for facial prostheses. Typically craniofacial implants are placed in the orbital (around the eye), the nasal, midfacial, and mastoid (behind the ear) regions. Typically, the implants are then connected by a metal superstructure which retains the prosthesis through a clip system. Alternatively, snap couplers or magnet systems, which do not link the implants, are used to retain the prosthesis.

For a prosthetic ear the typical retention system is a two implant bar and clip system shown in Figure 1-1. This retention system is usually comprised of the following components: two titanium flanged implants, which are implanted into the bone, two abutments, which are attached to the flanged fixtures via the abutment screws, a bar superstructure which consists of three bars welded or cast to two cylinders. The cylinders are fastened to the abutments via screws, as depicted in Figure 1-2. The prosthetic ear then clips to the bar superstructure.

There are some significant differences between intraoral and craniofacial implants. First, craniofacial implants are shorter with typical lengths of 3mm to 4mm in comparison to the intraoral implants which can be up to 20mm in length. In addition, a craniofacial implant has a flange above the threaded section of the implant. This flange aids in implant stability during the healing process and prevents tipping due to implant loading

(Brunski and Skalak, 1998). The other significant difference is craniofacial bone sites have anatomy that is different and more varied than that encountered in the intraoral bone sites.

1.1.3 Bone-Implant Interface

The long-term success of an implant is believed to be dependent upon maintaining a strong bone-implant interface (Brunski, 1992). After surgical insertion of the implant the interface developed depends on the healing processes of the surrounding bone. The remodeling/modeling of bone surrounding the implant can form an osseointegrated interface, which is an extremely strong and stable interface. There can also be development of fibrous tissue around the implant, believed to be a result of implant micromotion during healing (Brunski, 1992). This type of non-integrated interface generally leads to implant failure (Brånemark et al., 1985).

One test of implant stability and osseointegration that is used is the Periotest® (Siemens, BioResearch Inc., Milwaukee, Wisconsin). Originally designed to test the mobility of a tooth, the Periotest® is an electronic device that measures the stiffness properties of a tooth and converts this to a value representing mobility (Meredith, et al., 1998, May, et. al., 1997)). The Periotest® accelerates a metal rod toward the tooth, the time between the initial contact of the tooth and the time that the metal rod looses contact with the tooth (contact time) is measured and then converted to a Periotest® value (PTV). The PTV ranges from −8 to 50 and represents low to high mobility of the tooth respectively. In a study by May, the mean PTV for an accurately assembled abutment—implant connection -6.0 (May, et al., 1997). This study used intraoral implants placed in a bovine rib.

However, there are factors other than implant stability that affect the Periotest® values and as a result its clinical effectiveness is limited. A study by Meredith showed that the PTV changed dependent upon the striking height of the abutment and the handpiece angulation—both of which are hard to control in an in vivo environment (Meredith, et al., 1998).

1.1.4 Mechanical Loading

One of the main factors believed to affect the health of the bone-implant interface is the strain developed in the bone due to implant loading. There are many theories relating bone adaptation to strain. For example, Frost's mechanostat theory attempts to relate the type of response of bones that are normally load bearing to various levels of strain (Frost, 1987). According to this theory, strains that range from $100\mu\varepsilon$ to $300\mu\varepsilon$ represent the minimum effective strain (MES) for bone remodeling, which is the normal turn over of healthy bone. Strain below the MES for remodeling would result in bone loss or resorption. The MES for bone modeling, or the formation of new bone, is about $1500\mu\varepsilon$ to $2500\mu\varepsilon$, and bone fracture occurs approximately at $25000\mu\varepsilon$. The appropriate levels of strain for craniofacial bones are not known, but it is believed that the values would be lower considering these bones are normally relatively non-load bearing, and in the case that the bone quality has been compromised by disease or radiation treatment the values could be considerably lower.

The general belief that a certain level of strain is required for normal bone remodeling has led to the study of mechanical loading on implants. There are two main types of loads generated on osseointegrated implants. The preload generated by tightening the

prosthetic construction to the implants, and the functional or external loads generated during general daily functions. There have been various *in vivo* and *in vitro* studies done to determine the loading on oral implants. Two such studies were done using strain gauges attached to the abutment, turning the abutment into a load cell capable of measuring loads and moments. Glantz used this technique to determine the functional loading on oral implants *in vivo* and *in vitro* (Glantz, et al., 1993). In a study by Smedberg, strain gauges were used to determine the preload of the screw joint and the external preload generated on intraoral implants *in vivo* and *in vitro* when the superstructure was connected (Smedberg, et al., 1996). In Smedberg's study three different superstructures were used: a cast and milled bar superstructure, a cast superstructure covered by an outer heat cured denture based polymer, and a prefabricated laser welded titanium superstructure. However, very little work has been done on loads on craniofacial implants. One study by Del Valle measured the removal forces of various mechanical retention devices *in vitro*, ball and socket, magnets, and bar and clip. Removal forces varied from about 3N to 27N, dependent upon the retention system used and the method of removal (Del Valle, 1995). In an unpublished preliminary study measuring *in vivo* functional loading on craniofacial implants used to support an auricular prosthesis during various activities, such as eating, talking, removal and replacement of prosthesis (Faulkner and Berg, 1998). The results of this study identified the attachment and removal of the prosthesis as the only significant functional loads.

A gold screw tightened to about 10N·cm results in a preload of 250N to 300N in the screw joint (Rangert et al., 1991; Smedberg, et al., 1996). If the superstructure is 'non passive' (there are geometrical differences between the cylinder and abutment) an

external preload is added to the system, which could be transferred to the implant. In Smedberg's study, predefined misfits of 100μm were introduced by replacing the middle three abutments with shorter abutments and additional preloads of 200N were measured (Smedberg, et al., 1996).

It is important to note that the preload generated due to tightening the gold screw is dependent upon a number of factors such as geometry of components, friction, and applied torque. In a study by Burguete, the torque achieved by a Nobelpharma Torque Controler device was between 65% and 80% of the set torque at low speeds (Burguete et al., 1994). Further tests showed that repeated presses of the controller pedal at low speed resulted in an increase in achieved torque to values higher than the set torque of 10N·cm. Burguete's estimates on the preload of an unlubricated screw joint vary from approximately 250N for a torque of 7.5N·cm to over 400N for a torque of 12.5N·cm.

There are various clinical methods that have been developed for determining passive fit. Two such clinical methods are the one-screw test and the screw resistance test (Jemt, 1991). In the one-screw test, the superstructure was placed on the abutments and a gold screw was tightened at one of the abutments. The vertical gap between the other cylinder and abutment was observed. The screw resistance test was done be tightening each one of the gold screws until the first resistance was encountered. The gold screw was then tightened by a further 180°, a half a turn. If more than a half a turn was required to fully seat the superstructure on the abutments, it was considered to be a poor fit. Half of a turn corresponds to a vertical misfit of greater than 150μm, which is half of the pitch of a gold screw.

It is important to note, that although it is known that misfit introduces greater preload on the implants it is still uncertain whether or not it results in loss of osseointegration (Taylor, et al., 2000).

1.1.5 Biomechanical Models for Predicting Load Distributions Between Implants

Various theoretical engineering models have been developed to predict the loads generated on intraoral implants. The following is an overview of some of the main models developed, and the assumptions on which they are based.

1.1.5.1 Skalak

In 1983, Skalak developed a theoretical model for predicting the horizontal and vertical loads generated on implants connected by a rigid bridge (Skalak, 1983). In this model both the bridge and the bone are assumed to be infinitely rigid, and the implants are considered to be an elastic component with a known axial stiffness. In addition, Skalak assumes that the bridge is connected to the implants by a ball and socket joint, capable of supporting forces only.

1.1.5.2 Morgan & James

The 1995 Morgan and James model is capable of determining the force and moment distribution on dental implants (Morgan and James, 1995). Whereas previous models assume flexible joints, this model treats the connection between the implant and prosthesis as a rigid joint capable of transmitting both forces and moments. Once again, the bone and prosthesis are treated as rigid components with the only elastic component being the implant with a known axial stiffness.

1.1.5.3 Brunski & Hurley

The 1995 Brunski and Hurley model determines the distribution of forces and moments on implants supporting a bridge subjected to a vertical load (Brunski and Skalak, 1998). This model treats the implants as the elastic component with variable axial and bending stiffnesses. The bridge, and the connection between the implant and bridge are considered to be rigid.

1.1.6 Implant Stiffness

In the above biomechanical models, the implant was considered to be the elastic component. However, the bone-implant interface also has an effect on the overall stiffness. For example, for a 7mm Brånemark intraoral implant the axial stiffness changes from $4.55N/\mu m$ from to $2.50N/\mu m$ when it is inserted in trabecular bone (Brunski, 1992). In the load calculations done by Brunski, an implant stiffness of $11.0N/\mu m$ was used, which is in between stiffness values recorded *in vivo* and calculated from a Finite Element Analysis. A typical value for bending stiffness is $50000N \cdot mm/rad$ based on flexibility tests done by Rangert (Rangert and Gunne, 1991).

1.2 Thesis Outline

The purpose of this study is to develop an understanding of the loading situations on craniofacial implants. The loads and distribution of loads were measured both *in vivo* and *in vitro*, following the testing protocol outlined in Chapter 2. For the *in vitro* study, the preload generated when the superstructure was attached and the misfit in the superstructure, as determined by the one-screw test, were measured. For the *in vivo* case both the preload and functional loads were measured. Additionally, misfit of the

superstructure was assessed using the one-screw test. The functional loads measured were the replacement and removal of the prosthesis. These were considered to be the only functional loads of significance based on a preliminary test by Faulkner and Berg (1998).

Chapter 3 details the results of the experimental measurements and relevant comparisons. The relationship between superstructure misfit and preload is discussed, as well as the comparison between the *in vivo* and *in vitro* preload. The functional loads were compared to removal loads measured for bar and clip retention systems (Del Valle, 1995). In addition, the magnitude and distribution of functional loads on the implants was used to evaluate various biomechanical models.

The conclusions of the study are summarized in Chapter 4.
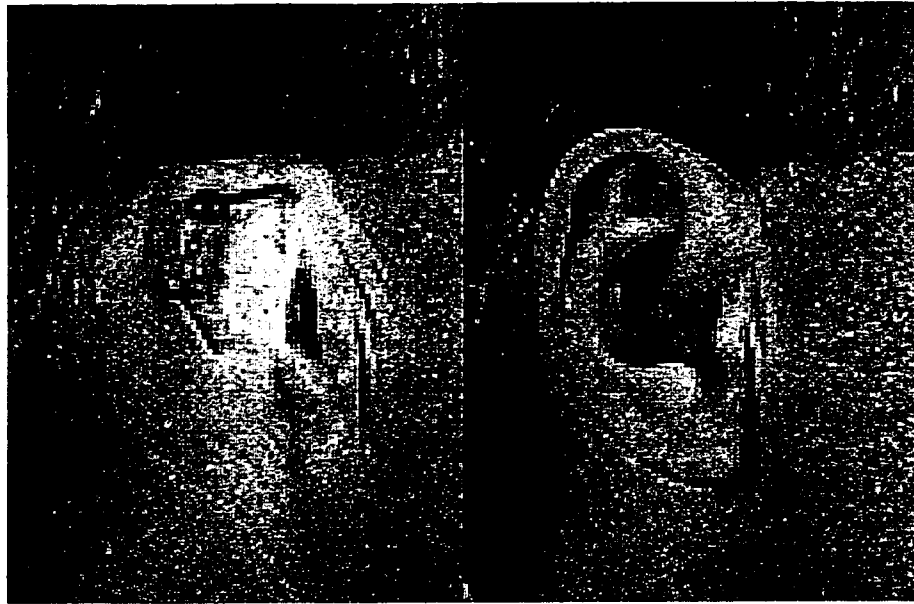
Figure 1-1: Implant Sites and Superstructure for Retention of an Auricular Prosthesis
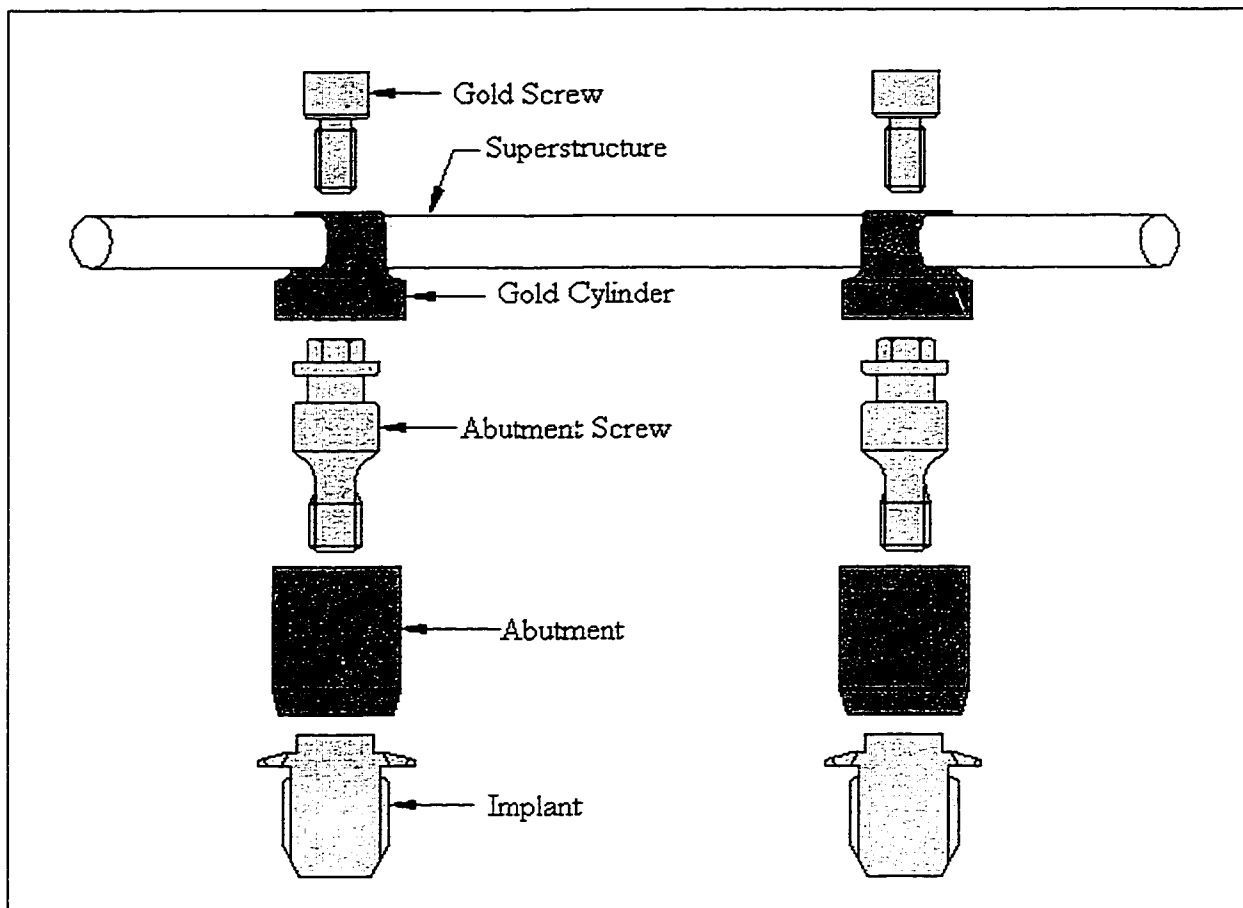
Figure 1-2: Components of a Bar and Clip Auricular Retention System

Chapter 2

Materials and Methods

2.1 Introduction

As previously discussed, for patients that are missing a portion of their head or neck due to disease or accident, osseointegrated implants are used to form the anchorage points for a structural superstructure which holds the silicone facial prosthesis. These implants must carry any loads generated by attaching the superstructure, loads that occur when the prosthesis is installed or removed—something which typically occurs at least once a day, and the loads developed while wearing the prosthesis. As the bone in which these implants are placed may have been compromised (for example by radiation therapy for cancer patients) the ability of the bone to remodel may be poor. Consequently the loads that the bone can safely carry are reduced, and so it is important to consider the loads that these implants carry. The intent of this study is to gain an appreciation of the loads and the distribution of the loads among craniofacial implant sites both *in vitro* and *in vivo*. As a model, for the present study the typical designs for an auricular (ear) prosthesis were considered.

2.2 *In Vitro* Testing

The *in vitro* strain testing consisted to two main parts: testing the preload generated when the bar superstructure was fastened into place, and measuring the vertical misfit of each of the bar superstructures.

2.2.1 Superstructure Construction Techniques

An acrylic test base along with superstructure materials were sent internationally to five separate craniofacial osseointegration centers: COMPRU (Craniofacial Osseointegration Maxillofacial Prosthetic Rehabilitation Unit) in Edmonton, Alberta, Canada; Morriston Hospital in Swansea, Wales; Queen Elizabeth Hospital in Birmingham, England; Institut Für Epithesen in Siegen, Germany; and Sahlgrens Hospital in Gothenburg, Sweden. The test base, shown in Figure 2-1, was a 10mm thick 100mm square acrylic block which contained the following components: two 4mm flanged implants (SEC 002, Entific Medical Systems, Gothenburg, Sweden), two 5.5mm standard abutments and abutment screws (SEC 007, Entific Medical Systems, Gothenburg, Sweden), and three bar positioner sections. The implants were placed 20 mm apart and an abutment was connected to each fixture by an abutment screw tightened to 20N·cm. The fixtures and abutments were secured using Loc-Tite®. The three bar positioner sections were placed in the test base to help with the construction of the superstructures. The superstructure materials that were sent to each of the five centers included: four 4mm gold cylinders (DCA 072, Entific Medical Systems, Gothenburg, Sweden), two hexagon head gold screws (DCA 074, Entific Medical Systems, Gothenburg, Sweden), and the

superstructure bar (CM-52028, Vident Canada, Mississauga, Ontario). The dimensions of the components used can be found in Appendix A.

Each fabrication center used their typical construction method to create two superstructures to fit the implant configuration that was sent. The bar for each superstructure was sectioned into three pieces, one to fit between the abutments and two cantilevers 10mm in length from the surface of the cylinder to the terminal end of the bar. These bars were then placed in the troughs of the bar positioners and then luted to the gold cylinders. The design of the superstructure bar was from center to center of the golds cylinders, this is referred to as a 'centric' design, as opposed to an 'eccentric' design where the bar section passes lateral to the gold cylinder. The bars were then removed and the superstructure was constructed and finished using the techniques specific to the fabrication location. The superstructures were then returned to COMPRU and the test base and materials were sent to the next center. A typical superstructure can be seen in Figure 2-2. The centers at Queen Elizabeth Hospital, COMPRU, Sahlgren's Hospital, and Morriston Hospital flame soldered the bar superstructures. The superstructures from Germany were different, as they were laser welded. More information on the framework construction techniques can be found in Table 2-1. In addition, COMPRU constructed a flame soldered eccentric superstructure, in which the bar was bent into shape instead of being sectioned. Consequently, this bar was soldered to the lateral side of the cylinder as shown in Figure 2-3. These prefabricated bar superstructures, hereafter referred to as the superstructures, were then used for the *in vitro* misfit and preload testing. Figure 2-4 shows the component labels that will be used.

2.2.2 Misfit Measurements

The superstructure misfit measurements were done using a Griffen and George cathetometer, which has an accuracy of $10\mu m$. The procedure used to test for misalignment mimicked the clinical one screw test. The test base was clamped into place, so that the front of the superstructure faced the cathetometer. The abutments were attached to the test base by the abutment screw, which was tightened to 20N·cm. The superstructure was positioned on the abutments and gold screw 1 was tightened to 10N·cm. The resulting vertical opening between abutment 2 and gold cylinder 2 was measured, as shown in Figure 2-5. This was repeated for a total of 3 trials. Next gold screw 1 was completely loosened and gold screw 2 was tightened to 10N·cm, and the resulting vertical opening between abutment 1 and gold cylinder 1 was measured. This was repeated for a total of 3 trials. These misalignment measurements were repeated for each of the eleven superstructures. The test base was then turned so that the cathetometer faced the back of the superstructure and the procedure repeated. This was to allow detection of any rotational misfit, meaning the gap was not constant but larger on one side.

2.2.3 Study Abutment

The abutments that were attached to the test base were modified to allow measurement of the loads being transmitted from the superstructure to the implants. The modified abutments will be referred to as the study abutments.

2.2.3.1 Design

Three linear strain gauges, type EA-06-015EH-120 (Micro-Measurements, Measurements Group Inc., Raleigh, North Carolina, USA), were mounted vertically on the outside of each abutment with an angle of 120° between gauges. In order to develop uniform strain sensitivity, the strain gauges were placed in a region where the cross sectional area of the abutment was constant, i.e. between the bottom inner lip and the top angled section of the abutment as illustrated in Figure 2-6. The strain gauges were attached using M-Bond 200 (Micro-Measurements) adhesive and then coated with M-Coat D acrylic (Micro-Measurements). This protective coating allowed the study abutments to be sterilized without damaging the strain gauges. The lead wires from each strain gauge were 0.005-inch diameter type 7X00157 (California Fine Wire, California, USA).

2.2.3.2 Calibration

To calibrate the study abutments a calibration base and calibration plate were made. The calibration base was an acrylic block with the same dimensions as the test base, but contained only one 4mm titanium flanged fixture positioned in the center of the base. The calibration system, shown in Figure 2-7 consisted of a calibration plate and a circular disk. The calibration plate was machined from 6061 Aluminum and had a gold cylinder attached to its center, and threaded holes tapped at 10mm intervals along its diameter. This calibration plate ensured that during the calibration process the study abutments were loaded in the same manner as in the *in vivo* and *in vitro* testing. The circular disk was used to apply the weights at a specific location on the calibration plate.

Each abutment was calibrated using the following method. One of the study abutments was attached, using an abutment screw, to the implant on the acrylic calibration base. The abutment screw was tightened to 20N·cm by a Brånemark System® DEA 020 Torque Controller (Entific Medical Systems, Gothenburg, Sweden). This is the controller that was used for tightening the abutment and gold screws during the calibration procedure and the *in vitro* testing, and will be referred to as the torque controller. The lead wires from each strain gauge were connected to an HP 1314A Data Acquisition System (HP) (Instrument Systems Corp., Edmonton, Alberta, Canada). The measurements from the data acquisition system were controlled and recorded using a calibration program written in HP VEE. The calibration plate was placed so that the gold cylinder was positioned on the abutment and the threaded holes of the calibration plate were perpendicular to the one of the strain gauges. The calibration plate was then secured into position using a washer and a calibration screw tightened to 10N·cm. The calibration screw was an eyeglass screw (McCray Optical Supply Mod.313 2.5mm Head). It was longer than a gold screw but had the same pitch and thread (dimensions can be found in Appendix A). After tightening the calibration screw a voltage reading for the unloaded condition was taken. The circular disk was then mounted into one of the threaded holes on the calibration plate and specific weights placed on it. The applied weight, the distance from the study abutment, and the resulting voltage for all three strain gauges was then recorded. Voltage measurements were recorded as the weights and the location of the circular disk were varied. This procedure was repeated three times, twice with the calibration plate's threaded holes perpendicular to a different gauge and once with the threaded holes parallel to gauge 1 (for calibration purposes, it was assumed that

gauge 1 was approximately aligned with the y-axis). The axial load, bending moment about the x-axis, and bending moment about the y-axis was calculated from the recorded data. A multiple regression was completed for each strain gauge to determine the moment and axial calibration constants. The theoretical background and equations used in this calibration procedure can be found in Appendix B.

2.2.4 Data Acquisition System

Each strain gauge was connected to quarter bridge circuit, which was monitored by a HP E1413A Data Acquisition System (HP). The HP monitored the gauge readings for both static *in vitro* and *in vivo* tests and the dynamic *in vivo* tests. Each strain gauge was connected to a separate channel on the data acquisition system, which allowed the HP to scan all six channels simultaneously. For the static measurements the HP was programmed to take 6400 scans during a 1 second period. To reduce the noise in the system the HP internally averaged every 64 readings to give a total of 100 readings per gauge for the 1-second time period. During the dynamic measurements, the HP was programmed to continually scan the channels until the user stopped the scans. For the dynamic measurements, 5000 scans were taken in a 1 second time period. Again the HP averaged every 64 readings to give a total of 78 readings per second.

2.2.5 Preload Testing

For the preload testing there were three preloads that were measured: the reference load, resultant load, and the misfit load. The reference load was the load generated in the abutment purely due to the fastening of the gold cylinder to the abutment via the gold screw, representing a perfect fit. This measurement was accomplished by turning the

superstructure so that only one of the gold cylinders was in place and the superstructure was completed supported by one abutment as shown in Figure 2-8. The resultant load was the load generated in the abutment when the superstructure was completely fastened into place, and the misfit load was the difference between the resultant load and the reference load.

For the preload testing, the two study abutments were fastened, via abutment screws, to the implants on the test base that they were originally attached to during the superstructure construction. The abutment screw was tightened to 20N·cm and the lead wires of the strain gauges were connected to the HP. All measurements were controlled and recorded using a static measurement program written in HP VEE.

There were four sets of measurements taken for each superstructure: a set of reference measurements for each abutment and a set of resultant measurements for each of the tightening sequences. Prior to each set of measurements the superstructure was completely removed and a zero reading was taken with only the abutments connected to the implants. The first set of measurements taken were the reference readings for abutment 1. The superstructure was positioned such that it was supported entirely by abutment 1 and then fastened into place by tightening gold screw 1 to 10N·cm. At this point two readings were taken, one immediately following the tightening of gold screw and one a minute later. The gold screw was than completely loosened, and the process was repeated 10 times, for a total of 20 measurements. Next reference readings for abutment 2 were taken following the same procedure as for abutment 1, except positioning the superstructure so that it was supported only by abutment 2. Then

resultant readings were taken for the first of the two tightening sequences. The superstructure was placed into position, and gold screw 1 was tightened to 10N·cm and then gold screw 2 was tightened to 10N·cm, this tightening sequence will be referred to as T1T2. Two readings were taken, one immediately following the tightening of gold screw 2 and then one a minute later. This was repeated 10 times for a total of 20 measurements. The last set of measurements was the resultant readings for the second tightening sequence and followed the same procedure as for the first tightening sequence, except gold screw 2 was tightened to 10N·cm and then gold screw 1 was tightened to 10N·cm, this tightening sequence will be referred to as T2T1. The reason that the both tightening sequences were tested was to determine if the misfit loads generated are influenced by the tightening sequence.

2.3 *In Vivo* Testing

The *in vivo* portion of the study was done at the COMPRU at the Misericordia Community Hospital and Health Center in Edmonton, Alberta. The study was approved by the Caritas Research Steering and Ethics Committee of the Caratis Health Group, Edmonton, Alberta. For the *in vivo* tests there were two types of loads tested: the preload generated when the superstructure was fastened into place and the dynamic loads generated when the prosthesis was attached or removed from the superstructure. There were four patients who participated in the study. Prior to patient testing the study was explained to each patient. Additionally, the patient was required to read a 'Study Information' sheet and then sign a consent form agreeing to participate in the study. These documents can be found in Appendix C. To reduce risk to the patient there was a selection procedure that was followed. Patients that participated in the study had

osseointegrated implants for an auricular reconstruction with only soft tissue surgery. The implants had to be installed for at least one year. Patients with a pacemaker, serious skin responses around the abutments, problems with the stability of the implants, or heart valve problems were excluded from the study.

2.3.1 Study Abutment

The study abutments used in the *in vivo* study at the COMPRU were the same study abutments that were used in the *in vitro* study. Before each of the patient testing the study abutments were disinfected by soaking them in Cidex for 20 minutes. The study abutments were removed from the Cidex and rinsed well in sterile water.

2.3.2 Testing Protocol

During *in vivo* testing, the patient's current prosthesis and superstructure was removed. Periotest® values were taken for the patient's original abutments. The patient's abutments were then removed and replaced with the study abutments (Figure 2-9), and the strain gauge lead wires were connected to the HP. The patient's superstructure was tested for 'misfit' by the clinical one-screw test as discussed in 1.1.4. The superstructure was placed on the abutments, gold screw 1 was hand tightened and gold screw 2 was left loose. The resulting gap between the abutment 2 and gold cylinder 2 was than observed. This was then repeated with the other gold screw 2 tight and gold screw 1 loose. Reference and resultant measurements were taken, following a similar procedure to that given in 2.2.5. However, due to time constraints with each patient, only four trials instead of ten were done for the reference measurements, for a total of eight measurements and three trials instead of ten were done for the resultant measurements,

for a total of six measurements. The superstructure positioning for the reference and resultant measurements are shown in Figure 2-10 and Figure 2-11 respectively. After completing the preload measurements, dynamic measurements were done to determine the external load applied when attaching or removing the prosthesis. A zero reading was taken with the superstructure attached, and then the six gauge readings were recorded continually while the prosthesis was put into place. Then, with the prosthesis in place, a zero reading was taken, and the gauge readings were recorded as the prosthesis was removed. This was repeated four times. The lead wires were then disconnected and the study abutments were replaced by the patient's original abutments. The patient's superstructure and prosthesis were attached and the patient was released.

Table 2-1: Superstructure Construction Techniques

Manufacturer	Flame Type	Preheating	Gold Screw (Torqued/Hand Tightened)
Queen Elizabeth Hospital Birmingham, England	Natural Gas	No preheating	Hand Tightened
COMPRU at the Misericordia Hospital, Edmonton, Alberta, Canada	Propane	500°C for 1 hour	Torqued to 10N·cm
Institut Für Epithesen Siegen, Germany	Laser Welded	No preheating required.	Hand Tightened
Sahlgren's Hospital Gothenburg, Sweden	Natural Gas	No preheating in oven, used flame for 15 minutes.	Hand Tightened
Morriston Hospital Swansea, Wales	Oxyacetylene	350°C for 1 hour	Torqued to 10N·cm
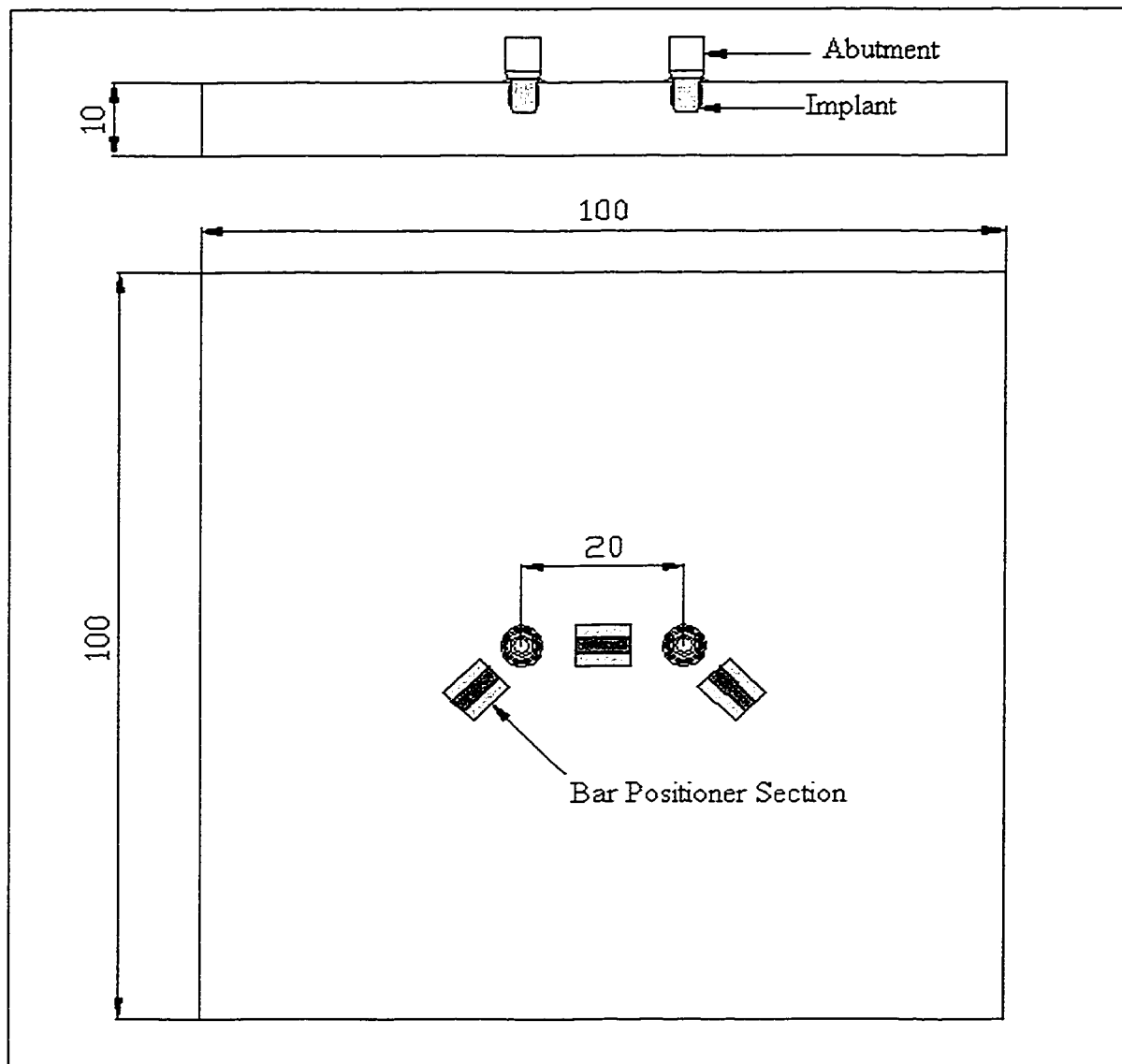
Figure 2-1: Test Base Sent to the Craniofacial Centers, Dimensions in mm
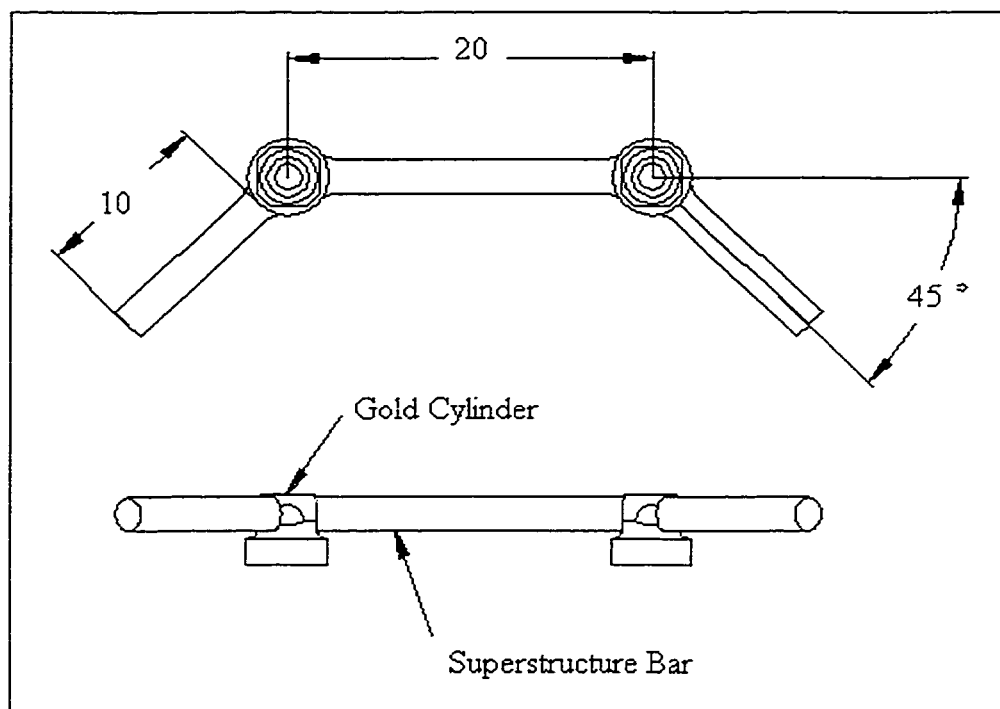
Figure 2-2: Typical Centric Prefabricated Bar Superstructure, all linear dimensions are in mm.
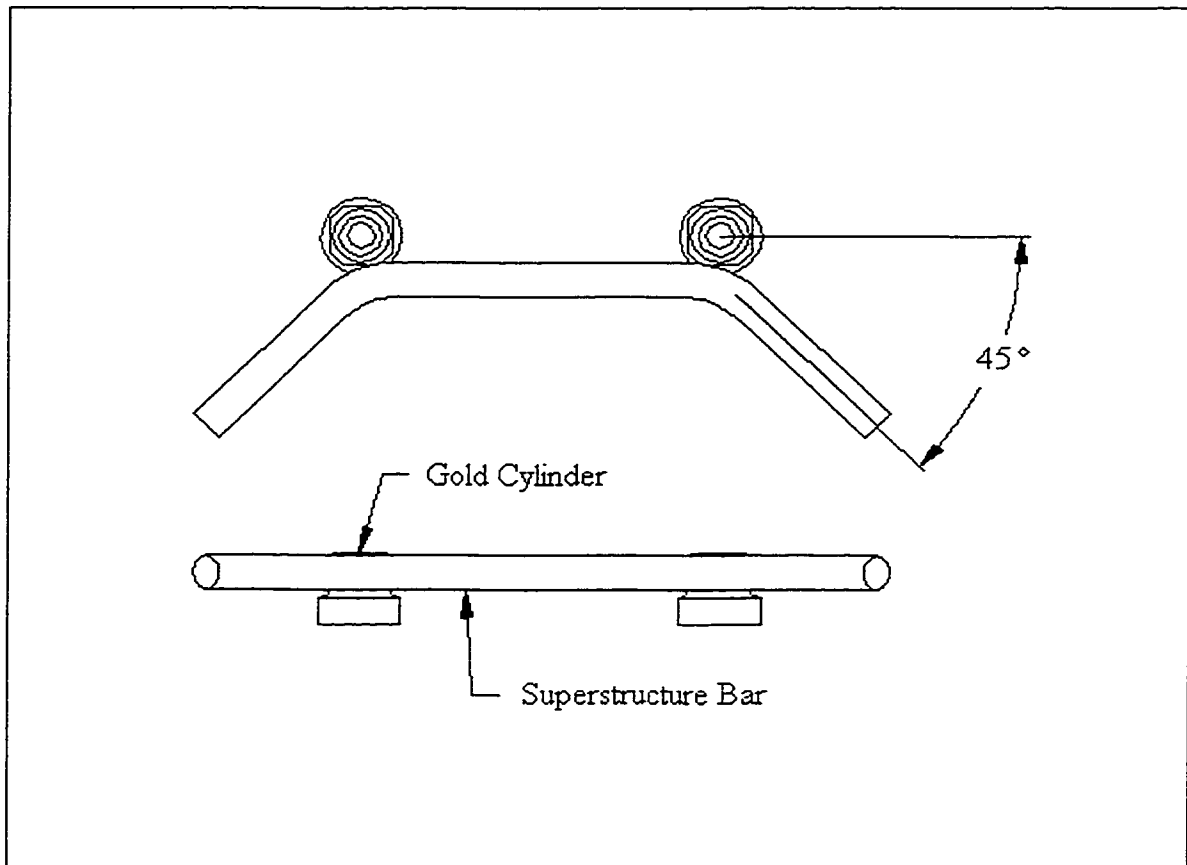
Figure 2-3: Eccentric Prefabricated Bar Superstructure.
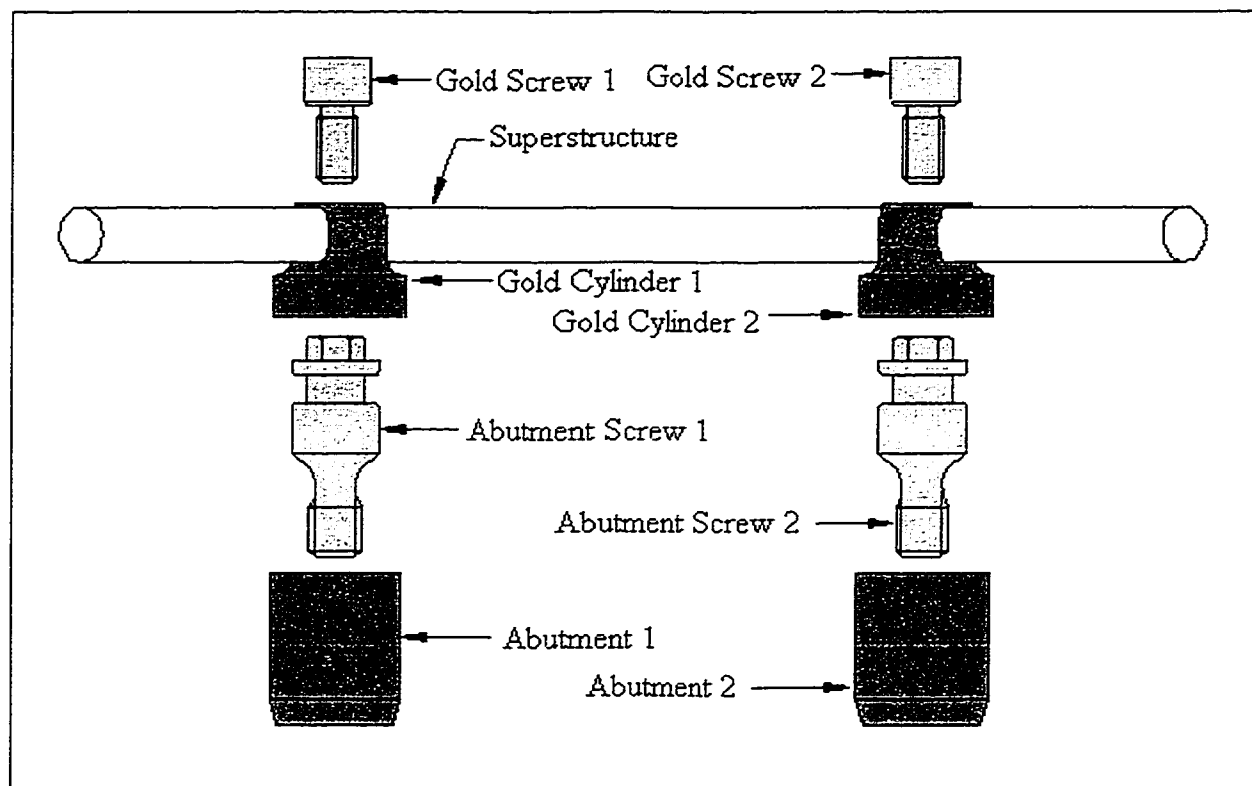
Figure 2-4: Component Labels
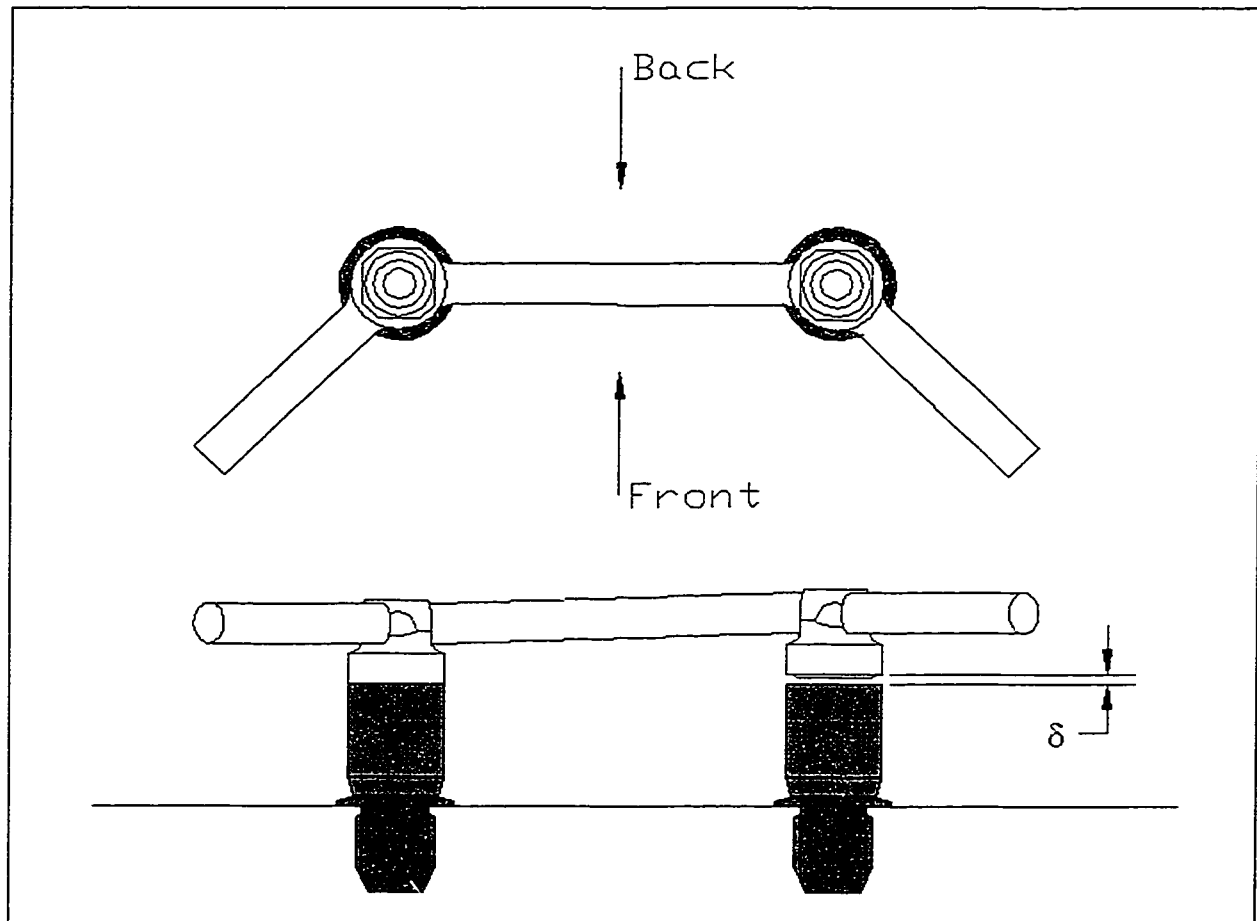
Figure 2-5: Vertical Gap Misfit Measurements
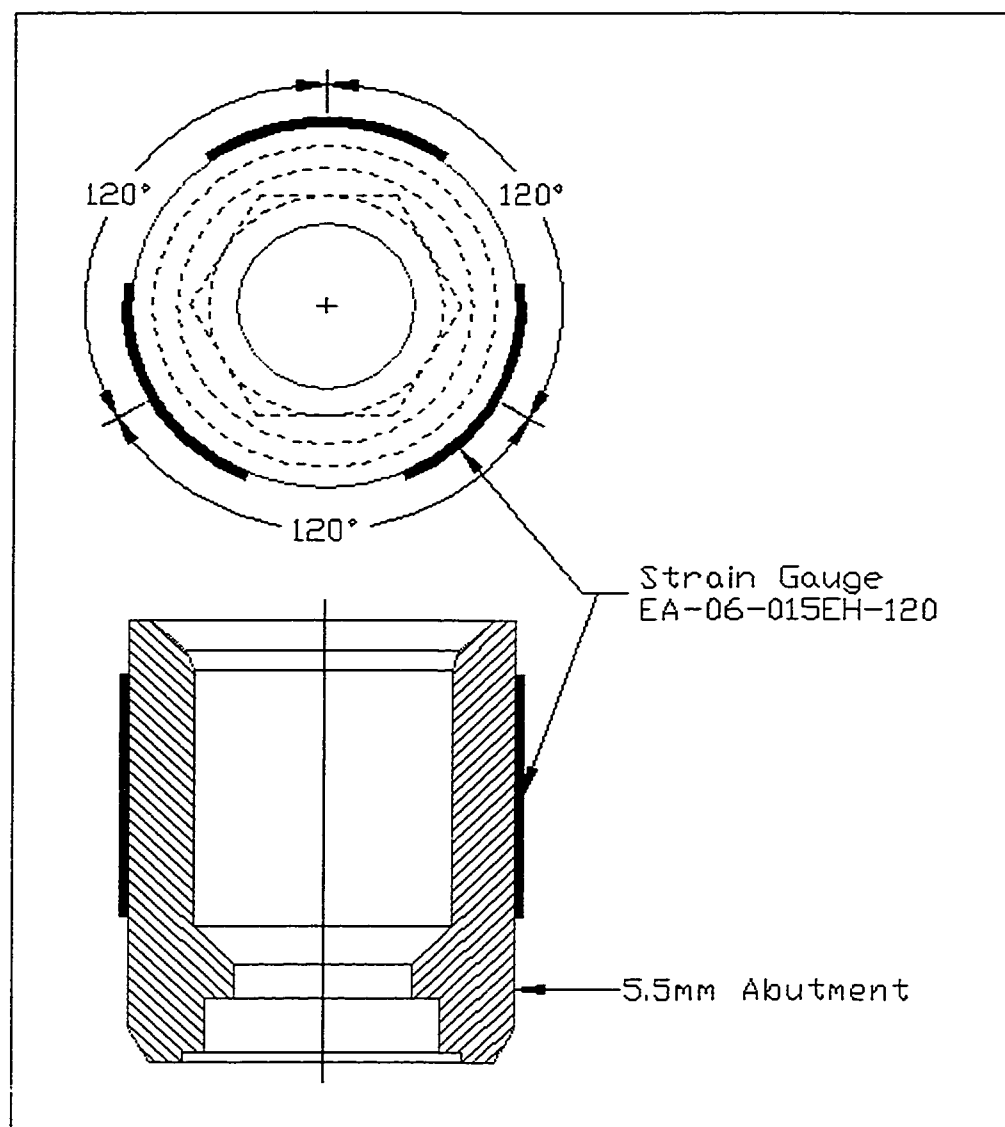
Figure 2-6: Strain Gauge Positioning on Study Abutment
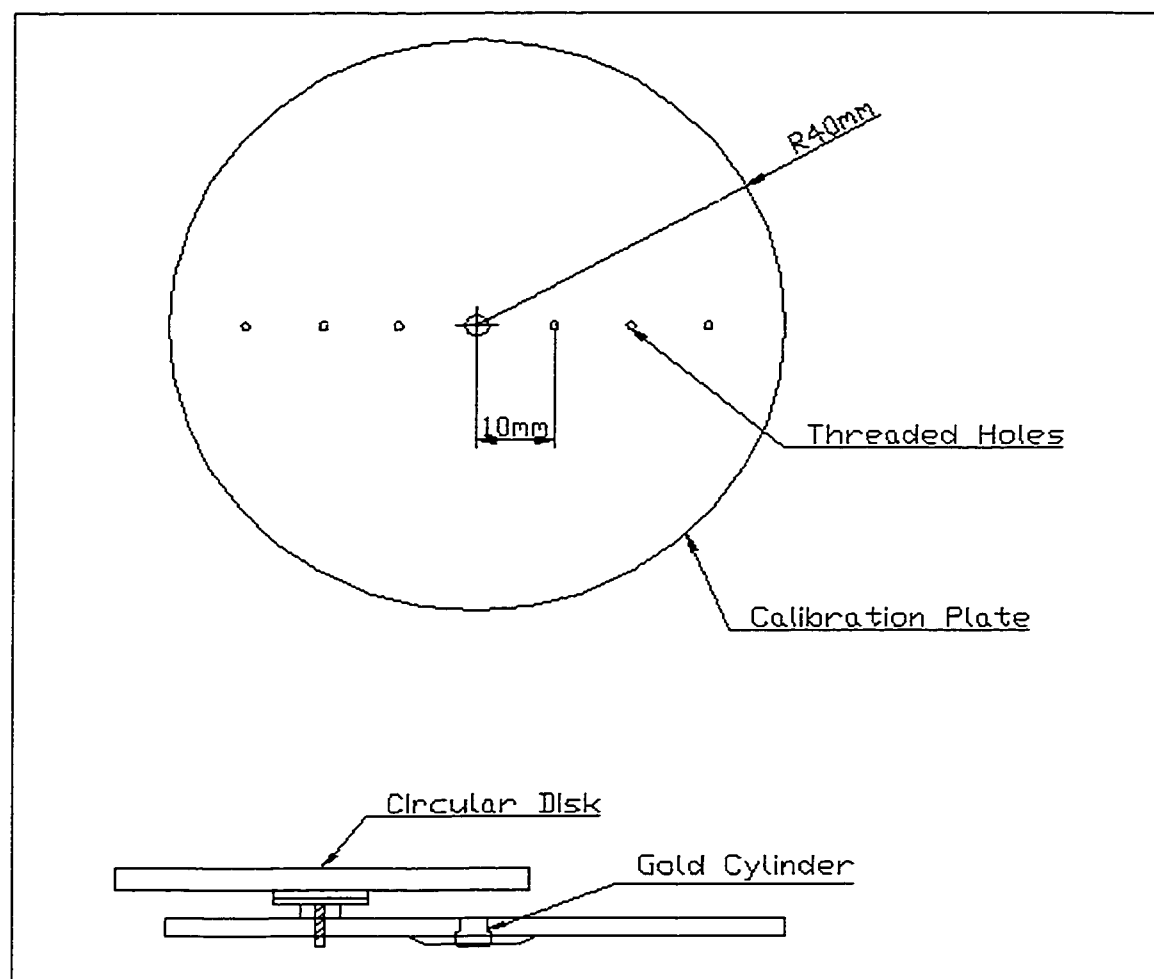
Figure 2-7: Calibration System
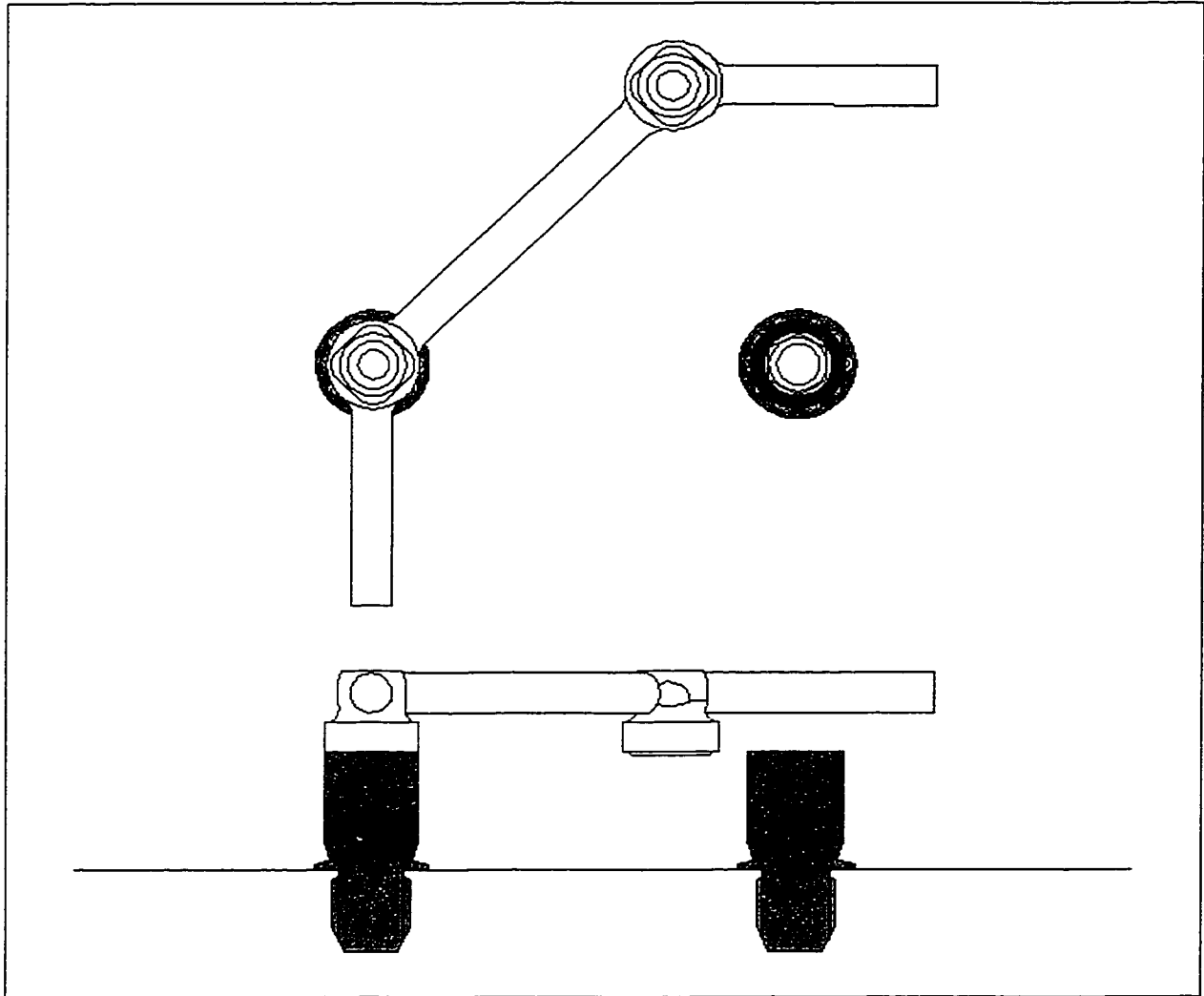
Figure 2-8: Positioning of Superstructure For Measuring Reference Load

Figure 2-9: Patient with Study Abutments Connected
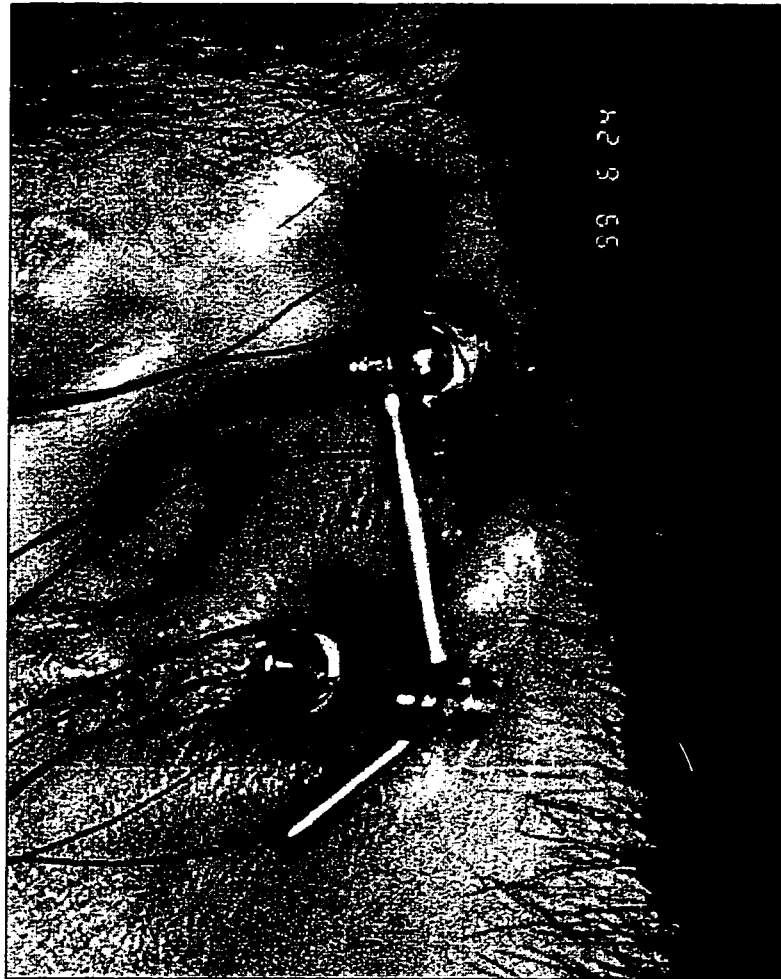
Figure 2-10: Superstructure Positioning for Measuring Reference Load
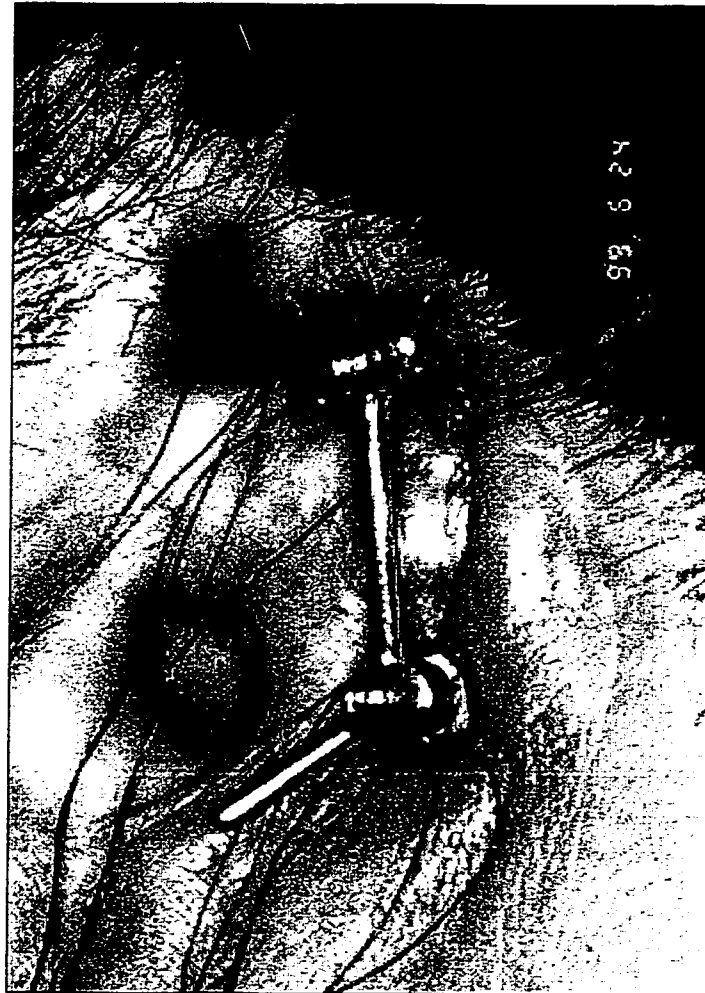
Figure 2-11: Attached Superstructure for Measuring Resultant Load

Chapter 3

Results and Discussion

3.1 Introduction

In this chapter, the experimental results for the *in vitro* and *in vivo* tests are shown. Using these results it was possible to determine whether there was a relationship between vertical misfit and misfit load, if there were significant differences between reference loads and resultant loads or significant differences between the loads generated for different tightening sequences. In addition, the results from the measured functional loads were used to evaluate different biomechanical models used to predict loads on implants.

3.2 *In Vitro*

There were eleven superstructures that were used in the misalignment and pre-load study. Table 3-1 provides some details of the superstructures as well as the designation that will be used for each. The free body diagram showing the forces on the retention system components can be found in Appendix D.

3.2.1 Misfit Measurements

Each of the eleven superstructures was optically measured for misfit by tightening one gold screw and measuring the resulting vertical gap between the other abutment and the superstructure. The vertical gap was measured from both the front and back in order to determine whether or not the gap was constant, or varied around the abutment. The results for each set of gap measurements were averaged and are shown with the standard deviation of measurements in Table 3-2. The vertical gap was compared to the clinically acceptable misfit level of 150μm (Jemt, 1991). Superstructures that had vertical gap measurements larger than 150μm were considered to be 'non-passive', while superstructures with vertical gap measurements less than 150μm were considered to be 'passive'.

The vertical gap ranged from 10μm to 290μm. As can be seen, most of the gaps varied from front to back indicative of some rotational misfit in addition to the vertical misfit. For example, the gap above abutment 1 varied from 40μm to210μm and from 30μm to 190μm for BIR1 and COM2 respectively. The following superstructures were considered to have a passive fit: BIR2, COM1, GER1, GOT2, WAL2. There was no correlation found between the superstructure construction techniques and the measured vertical misfit. It should be noted that these are vertical misfit values and do not take into account any rotational misfit or horizontal misfit of the superstructure.

If we approximate the superstructure as a cantilever beam with a constant circular cross section of 2mm, the theoretical force required to deflect the end of the beam can be calculated. The required force is dependent upon the material properties and dimensions

of the superstructure bar and the length of the cantilever beam. The length from the center of one gold cylinder to the other is 20mm and the superstructure bar is soldered between the gold cylinders. As a first estimate the effective length of 20mm was used, however, when the gold cylinders are considered the actual length of the bar is only 15.5mm. In addition, the welds that join the bar to the gold cylinders can also change the effective length of the bar. Figure 3-1 shows the theoretical force required to close the vertical gap for three effective lengths as calculated from the following equation

$$P = \frac{3\delta EI}{(L_E)^3},$$ (3-1)

where P is the force, δ is the vertical gap distance in μm, E, I and L_E are the modulus of elasticity, moment of inertia, and effective length of the 'beam' respectively.

3.2.2 Pre-Load

The pre-load measurements were done *in vitro* to determine the loads inherent to the retention system and the loads generated by connecting the superstructure. The preload is comprised of two parts, the load generated when the gold cylinder is attached to the abutment and the load generated due to any misfit of the superstructure. The measurements for each superstructure were averaged and are shown with a 95% confidence interval. Only the magnitudes of the bending moments are shown.

The reference axial force and bending moment for the eleven superstructures evaluated are given in Table 3-3. The reference axial force varied from –233N to –348N for abutment 1 and –250N to –367N for abutment 2. The overall average for the reference axial force was -290N, this is comparable to the expected screw joint preload of –250N to –300N generated when the gold cylinder is attached to an abutment by a gold screw

tightened to 10N·cm (Rangert, et al., 1991). The reference bending moment for abutment

1 varied from 7.0N·cm to 21.9N·cm and from 3.2N·cm to 28.2N·cm, excluding BIR2, for

abutment 2. The average reference bending moment was 11.7N·cm, which is relatively

low, as expected. The reference bending moment on abutment 2 for BIR2 was excluded

because during construction some of the soldering material flowed into the lip of the gold

cylinder, and as a result the gold cylinder did not sit flat on the abutment. As a result,

there was a bending moment of 69.7N·cm generated when the gold cylinder was attached

to the abutment.

The resultant measurements for the tightening sequence T1T2 and T2T1 are shown in

Table 3-4 and Table 3-5 respectively. The P and NP shown in brackets after each

superstructure designator represent passive and non-passive fit. The numbers in brackets

in the tables show the misalignment load, which is resultant load minus reference load,

with a 95% confidence interval. If no value is present this indicates that there was no

statistical difference between the resultant and reference measurement at the 5%

significance level. The resultant axial force varied from −163N to −377N for tightening

sequence T1T2 and from −227N to −362N for tightening sequence T2T1. The resultant

bending moments, again excluding BIR2 abutment 2, varied from 3.1N·cm to 45.1N·cm

and 3.1N·cm to 38.2·cm for tightening sequence T1T2 and T2T1 respectively. As

expected, connecting the superstructure to both abutments changed the preload in the

abutments, increasing it in some cases and decreasing it in others. Recalling that the

optimum preload ranges are from −250N to −300N, there are two situations that can

occur when the superstructure is tightened to both abutments. The magnitude of the

resultant load could be less then the optimum preload range, meaning a compressive

force less than 250N was measured and the desired clamping force is not achieved. Alternatively, the magnitude of the resultant load could be greater than the optimum preload range, meaning a compressive force greater than 300N was measured. In this later case there are higher loads in the components. Both cases have the potential of causing mechanical problems, whether it is screw loosening, fracture of components, or possibly implant failure. However, when the 95% confidence interval is taken into account most of the resultant axial forces fall into the optimum preload range as shown in Figure 3-2 for tightening sequence T1T2 and in Figure 3-3 for tightening sequence T2T1. The exceptions are BIR1 and COM1 for both tightening sequences and GER2 for tightening sequence T1T2. In the case of COM1 and GER2, the compressive force is less than the optimum and for BIR1 the compressive force is greater than the optimum preload.

The significant misfit axial force varied from −78N to 117N and from −69N to 76N for tightening sequence T1T2 and T2T1 respectively. As can be seen, there is not the expected correlation between vertical misfit and misfit load. It was expected that larger vertical misfit measurements would result in greater misfit loads. However, for tightening sequence T1T2, GOT2, which had a maximum vertical gap of 100μm, had a misfit axial load of −75N on abutment 1 and −41N for abutment 2. In contrast, COM3, which had a maximum vertical gap of 290μm, had a misfit load of −78N for abutment 1 and −31N for abutment 2. In addition, some of the 'passive' superstructures showed larger misfit load than the 'non-passive superstructures. For example COM1, for tightening sequence T1T2 has a misfit load of 67N on abutment 2. Furthermore, for superstructures that had a large vertical misfit as well as a larger misfit load, the misfit

load was larger than the force required to close the vertical gap. Even assuming an effective length of 12mm, the force to close the maximum vertical gap for BIR1, which was 210µm, would have been -28N but the misfit load was −77N.

It is important to note that only the vertical misfit was measured, each of these constructed superstructures could have both horizontal as well as rotational misfit, both of which could significantly alter the misfit load. Although measuring the vertical gap from both the front and back of the superstructure showed that most of the superstructures had some rotational misfit, it was not possible to determine the magnitude of the misfit. As an example, GOT2 had one of the largest misfit loads but was considered to have a passive fit. However, GOT2 had a vertical gap that varied from 10µm to 40µm from front to back on abutment 1 and from 100µm to 30µm front to back on abutment 2. Assuming that the front and back were the locations of the minimum and maximum gap, gold cylinder 1 was slightly tilted to the front while gold cylinder 2 was tilted toward the back. Consequently, when tightening the forces had to both bend the superstructure to close the vertical gap as well as twist the superstructure to close the rotational misfit. As a result, the measured misfit loads would have been larger than those expected based on the vertical misfit. Additionally, the misfit load is partially depended upon the applied torque; consequently variations in the applied torque by the torque controller would also have an effect on all of the measured loads.

The significant misfit bending moments varied from −6.4N·cm to 27.1N·cm for tightening sequence T1T2 and from −6.3N·cm to 24.4N·cm for tightening sequence T2T1. The magnitudes of most of the misfit moment loads are low, less than 13N·cm.

The exceptions are COM3, GER2 and WAL1, all of which were 'non-passive' superstructures. Once again, the misfit moment load was independent of the vertical misfit.

It should be pointed out, that although there was no direct relationship between the magnitude of the vertical misfit and the resulting misfit load, all of the non-passive fits did have a significant misfit load, whether it was a significant axial load as with BIR1, or a significant moment load as with WAL1, or both as in the case of COM3.

Table 3-6 shows the difference between the two tightening sequences at the 5% significance level. For all of the superstructures, the tightening sequence affected the resultant load. It was expected that the difference in the vertical misfit between abutments 1 and 2 would result in a corresponding difference in the tightening sequence, meaning a larger difference between the gap above abutment 1 and the gap above abutment 2 would indicate a difference in tightening sequences. However, COM1, which had the smallest difference between the maximum gap above abutment 1 ($30\mu m$) and the maximum gap above abutment 2 ($70\mu m$), had a difference between tightening sequences of 65N and 43N for abutment 1 and 2 respectively. The difference in tightening sequence for the resultant bending moments was small for all of the superstructures, varying in magnitude from 0 to 7.6N·cm. Once again, although the difference in tightening sequences could not be accounted for by the vertical misfit, there are other factors, such as variation in applied torque or rotational and horizontal misfit that cannot be accounted for.

Although the one-screw test is an easy measure of clinical misfit, caution should be used when determining the passivity of the superstructure using this method. This test only accounts for vertical misfit and neglects other forms of misfit, which may be of more of a concern.

3.3 *In Vivo*

Table 3-7 gives some background information on each of the four patients that participated in the *in vivo* portion of the strain gauge study done at the COMPRU at the Misericordia Hospital in Edmonton. The four patients, who participated in this study, all had auricular prostheses and will be referred to by the labels: AB, CB, HB, and SF. The dimensions and shape of the patient superstructures and the location of the two study abutments are shown in Figure 3-4.

3.3.1 Pre-Load

Prior to pre-load testing the patient's superstructure was clinically tested for 'misfit' using the clinical one-screw test, as discussed in 2.3.2. According to the clinician, there was very little gap between the gold cylinder and abutment when either gold screw was tightened—all four superstructures were considered to be a 'passive' fit. In addition, Periotest® values (PTV) were taken for the patient's original abutments, the PTV for each abutment is shown in Table 3-8, and ranged from –5 to –7, which is comparable to the typical PTV of approximately –6.0 (May, et al., 1997)

The pre-load testing was done to determine the amount of load generated by attaching the superstructure to the abutments. Due to the limited testing time with each patient there were a total of eight measurements made for each reference load and six for each of the

two tightening sequences. The mean and standard deviation were calculated for these measurements.

The reference loads measured for the *in vivo* tests are shown in Table 3-9. The reference axial force ranges from –260N to –492N, while the bending moments range from 5.0N·cm to 17.1N·cm. The axial force results are higher than the reference axial forces measured in the *in vitro* testing, which ranged from –233N to –367N, but comparable when the error in the *in vivo* measurements is considered. The bending moments are similar to those measured *in vitro*, which ranged from 3.2N·cm to 28.2N·cm.

Table 3-10 and Table 3-11 show the resultant loads measured for the tightening sequence of T1T2 and T2T1 respectively. The values in brackets are the misfit loads (i.e. resultant load minus reference load) with a 95% confidence interval. If no value is present there was no statistical difference between the resultant and reference loads at the 5% significance level. The resultant axial force varied from –194N to –468N for tightening sequence T1T2 and from –192N to –426N for tightening sequence T2T1. The significant axial misfit loads varied from –72N to 129N, however, the confidence intervals for these values were quite high in comparison to the approximately 38% to 74% of the misfit load. Figure 3-5 shows a comparison between the reference axial force and the resultant axial force for the two different tightening sequences for patients AB, CB, HB, and SF. The error bars show the standard deviation of the data. As can be seen, when the standard deviation in the measurements is considered, there is little difference between the reference and resultant measurements for the axial force (i.e. the superstructure is a good fit). The resultant bending moments varied from 4.1N·cm to 28.0N·cm for

tightening sequence T1T2 and from 4.8N·cm to 27.7N·cm for tightening sequence T2T1.

The difference in the resultant and reference bending moment, bending moment caused

by misfit, varied from –7.0N·cm to 18.3N·cm. Figure 3-6 shows a comparison the

reference and resultant bending moments for patients AB, CB, HB and SF. All patients

showed a significant difference between the reference and resultant bending moment

measurements.

Table 3-12 shows the difference in the resultant measurements for the tightening

sequences T1T2 and T2T1. There is a significant difference in the axial force for the two

tightening sequences for at least one abutment for all three out of four patients. The

differences range from –37N to –87N; however the confidence levels on these values are

high, 49% to 59% of the measured values. Patients AB abutment 1 and CB abutment 1

and 2 show a significant difference in resultant bending moments for the two tightening

sequences, but the differences are small, 3.1N·cm to 6.3N·cm. The tightening sequence

had no significant effect on the resultant bending moment for the rest of the patients at

the 5% significance level.

3.3.2 Functional Loads

As previously mentioned there were two functional loads that were measured *in vivo*: the

load generated during the attachment of the prosthesis and the load generated during the

removal of the prosthesis. Since there were only four trials done for each of the two

functional loads tested, the results were not averaged for each patient and the error stated

is the estimated error in each individual measurement. Due to the significant level of

electrical noise in the raw data from the six gauges, the results for the axial loads are not

reliable, but have been included. (The study abutments are more sensitive to a bending moment than a axial force, consequently noise in the gauge readings results in small fluctuations in bending moments and large fluctuations in axial loads.) The error in the individual measurements for each abutment was determined using a sensitivity analysis. The regression equations (Appendix B) were used to determine the effect the fluctuations in the gauge readings had on the calculated axial force and bending moment. However, in order to reduce the noise in the raw data, the data was run through an averaging program. As a result the averaged data had significantly less noise then the original data. The standard deviation of the raw data was approximately $20\mu V$ whereas the standard deviation of the averaged data dropped to about $2\mu V$. If the standard deviation of the averaged gauge readings was used in the sensitivity calculation the error was considerably reduced. For example, for the raw data for replacement 1 for patient SF the axial and bending moment error are $\pm32N$ and $\pm0.5N\cdot cm$ and $\pm21N$ and $\pm1.0N\cdot cm$ for abutments 1 and 2 respectively. If the averaged data is used these errors drop to $\pm5N$ and $\pm0.1N\cdot cm$ and $\pm2N$ and $\pm0.2N\cdot cm$ for abutments 1 and 2 respectively.

3.3.2.1 Replacement of the Prosthesis

Each prosthetic ear contained three clips, one for the middle bar of the superstructure and one for each of the cantilevers. During the replacement of the prosthetic ear the clinical assistant lined up the clips to the superstructure and pushed them into place, while the gauge readings was continuously recorded. This recorded data was then used to calculate the axial force and the magnitude of the bending moment generated on each abutment during the replacement of the prosthesis. The maximum and minimum axial force generated during the replacement of the prosthesis is shown in Table 3-13. The axial

force varies from –51N to 26N. As indicated these axial values have considerable uncertainty. The maximum bending moment generated is shown in Table 3-14. The maximum bending moment generated during the replacement of the prosthesis varied from 2.8N·cm to 37.3N·cm. The values shown in these tables are the absolute maximum and minimum during the replacement of the prosthesis and although it quantifies the results it does not give a clear picture of the how the loads vary during the replacement of a prosthetic ear.

It is important to remember that the replacement of the prosthesis was done manually by a clinical assistant, and it was difficult to attach the prosthesis in the same manner for each trial. There were three clips that had to be lined up and connected and the force exerted by the clinical assistant varied dependant upon the sequence in which the clips were engaged. As a result, each replacement was unique, with the axial load and bending moment reflecting the forces exerted on the prosthesis with considerable variance between patients as well as the individual trials. Figure 3-7 and Figure 3-8 show how the axial force and bending moment varied during a prosthesis replacement for two different trials for the same patient. In replacement 1 (Figure 3-7) the maximum bending moments for abutment 1 and abutment 2 both occurred at approximately 3.6 seconds, at this point the axial force on abutment 2 was at a minimum and the axial force on abutment 1 had a local minimum of about –16N. The minimum axial force on abutment 1 occurred at about 4.5 seconds at which point there was a local minimum force on abutment 2 and local maximum bending moments on both abutments. There was a local maximum axial force on abutments 1 and at 4 seconds of –7.5N and 1N respectively. In addition, the loads on the abutments did not fall back to zero after the prosthesis was in place. This

indicates that the prosthesis adds a load to the system that is present as long as the prosthesis is in place. For the second replacement (Figure 3-8) the maximum bending moment for abutment 1 occurred at 3.3 seconds, at which point there is a minimum axial force of $-25N$ on abutment 2 and a local maximum of $-10N$ on abutment 2. The maximum bending moment on abutment 2 occurred at approximately 2.7 seconds, at which point both the axial force on abutment 1 is decreasing and the axial force on abutment 2 is increasing. The minimum axial force on abutment 2 occurs at about 1.9 seconds and at that time there abutment 2 has local maximum bending moment of about $10.5N \cdot cm$.

3.3.2.2 Removal of Prosthesis

As with the replacement of the prosthesis, the removal was done by the clinical assistant while the gauge readings were continuously recorded. The gauge readings were then used to calculate the axial force and bending moment on the two abutments. The results for the maximum and minimum axial force generated during the removal of the prosthesis are shown in Table 3-15. The maximum axial force generated during the prosthesis removal ranged from 4N to 30N, while the minimum axial force ranged from 0N to $-14N$. The average maximum force required to remove the prosthesis was 24N was comparable to the vertical removal forces of 15N to 23N for a three retention point bar and clip system (Del Valle, 1995). Both the error in the axial measurements as well as the tightness of the clips can account for these higher values. The maximum bending moment generated on the abutments during the removal of the prosthesis is shown in Table 3-16, and vary from $3.4N \cdot cm$ to $20.5N \cdot cm$.

The removal of the prosthesis could be accomplished in three ways. The prosthesis could be pulled off using an axial force with very little moment, which would be identified by high axial forces and low bending moments. For example, the maximum axial force for patient HB for the four trials varied from 15N to 28N while the bending moments varied from 3.4N·cm to 5.8N·cm. Alternatively, the prosthesis could be removed be lifting one edge of the prosthesis, or removing the prosthesis mainly with a moment, which would result in high bending moments and low axial forces. Patient CB had a maximum axial force that varied from 4N to 14N for the four trials while the bending moment varied from 6.2N·cm to 11.1N·cm. In the third method, the prosthesis would be removed by a combination of a pull and lift, which would have higher axial forces and bending moments. Patient AB had both high axial forces on abutment 1, 21N to 28N, and low axial forces on abutment 1,4N to 10N. The bending moments for these four trials were high and varied from 11.9N·cm to 20.5N·cm. Trial 2 for patient SF also falls into this category.

Since the removal of the prosthesis was easier for the clinical assistant to do, there is more consistency between trials of the same patient. Figure 3-9 and Figure 3-10 show the axial force and bending moment during the removal of the prosthesis for patient AB's trials number 2 and 4 respectively. In both trials, the bending moment generated on the two abutments has the same shape as it increases to a maximum, with the maximum bending moment greater on abutment 2. The maximum axial force on abutment 2 occurs at the same point in time as the maximum bending moment, while the axial force on abutment 1 does not hit an obvious peak, but fluctuates between –5N and 5N. Figure 3-11 and Figure 3-12 show the axial forces and bending moments generated on the

abutments during the removal of the prosthesis for patient CB, trials 1 and 2 respectively. Once again the bending moments generated on the two abutments followed the same shape and increased to a maximum value, with the maximum bending moment on abutment 2 greater than that on abutment 1. However in these cases at the point of maximum bending, the axial force on abutment 1 was at a maximum, but at a minimum on abutment 2.

It should be noted that in all of the removal graphs, the bending moments follow the same path, but with different magnitudes. This could indicate that the stiffnesses of the two implant sites were not equal. Since the implants are identical, this difference in stiffness could be dependent upon type or thickness of the bone that the implant is placed in, or the bone-implant interface. There is no relationship between the Periotest® values for the abutments and which abutment sees the larger moment. Patient AB had a abutment 2 had the higher bending moment and the lower PTV, whereas for patient SF abutment 1 had the higher bending moments and the higher PTV.

3.4 Predictions of Forces and Moments on Implants

The Skalak model and the Brunski and Hurley (BH) model were used to determine the forces generated on the abutments during the removal of the prosthesis from the superstructure of patient AB. The Morgan and James model was not used due to the fact it produces the same results as the BH model, assuming that the axial stiffness of the implants are the same. The superstructure had three activation points at the midpoint of each superstructure bar, where the prosthesis was attached via a clip, as shown in Figure 3-13. The coordinates of the implants and the activation points are shown in Table 3-17.

The removal bending moment was assumed to be approximately 20N·cm, from *in vivo* results. The removal force was assumed to be 20N (Del Valle, 1995). In the first case the 20N force was evenly distributed between the activation points. In the second case the 20N force was distributed so that removal of the prosthesis was done by a moment only. In the third case, the 20N force was distributed so that the removal of the prosthesis was by a force and a bending moment. The forces are applied at the three activation points for the three cases are shown in Table 3-18.

As a first approximation the axial stiffness of the implant sites was taken to be 11000N/mm and the bending stiffness was taken to be 50000N·mm/rad (Brunski, 1991). The resulting forces on implants 1 and 2 using Skalak's model and the BH model are shown in Table 3-19. As can be seen there is little difference between the force predictions using the two separate models. This is due to the fact that the same axial stiffness was used for both implants for the BH model. The predicted axial forces ranged from −0.8N to 10.9N in comparison to the axial forces of 4N to 30N measured *in vivo*. The BH model predicted bending moments on the two implants of 3.3N·cm for case 1, 10.0N·cm for case 2 and 3. The predicted moments were the same for each abutment since they were considered to have the same bending stiffness; however, the bending moments measured *in vivo* varied from 3.4N·cm to 20.5N·cm. Skalak's model cannot predict bending moments due to its assumption that the connections are ball and socket joints; as a result the BH model has more value to the craniofacial situation. If the two implants have equal axial and bending stiffnesses, the BH model predicts that the axial force is fairly evenly distributed between the two implants and the bending moment is equal for the two implants. The *in vivo* results show that the forces are not evenly

distributed nor are the bending moments the same, suggesting that the implant site stiffnesses are different.

In order to determine whether changing the stiffnesses in the BH model would correctly predict the load distribution on the implants, the actual removal force and moment had to be estimated. For the first removal of the prosthesis for patient AB, the following loads were measured: abutment 1 had an axial force of 9N and a bending moment of 14.2N·cm, abutment 2 had an axial force of 21N and a bending moment of 20.5N·cm. Using the equations of static equilibrium, the forces applied to the three activation points had to equal an axial force of 30N and a bending moment of 34.7N. Therefore, the estimated removal forces were: 31N at activation point 1 and 3, and −32N at activation point 2. These loads were then used in the BH model. It was found that by changing the stiffnesses it was possible to predict the measured loads on implants 1 and 2. For example, if the axial and bending stiffness for abutment 1 was set at 200N/mm and 34500N·mm/rad and the axial and bending stiffness for abutment 2 was set at 2500N/mm and 50000N·mm/rad the predicted loads were similar to the measured loads. Other combinations of stiffnesses could also predict the measured loading, so the above numbers are not necessarily the correct stiffnesses.

Table 3-1: *In Vitro* **Superstructure Data**

Manufacturer	Sample #	Superstructure Type	Superstructure Name
Queen Elizabeth Hospital Birmingham, England	1	Centric	BIR1
	2	Centric	BIR2
COMPRU at the Misericordia Hospital Edmonton, Alberta Canada	1	Centric	COM1
	2	Centric	COM2
	3	Eccentric	COM3
Institut Fúr Epithesen Siegen, Germany	1	Centric	GER1
	2	Centric	GER2
Sahlgrens Hospital Gothenburg, Sweden	1	Centric	GOT1
	2	Centric	GOT2
Morriston Hospital Swansea, Wales	1	Centric	WAL1
	2	Centric	WAL2

Table 3-2: *In Vitro* **Misalignment Measurements**

Superstructure	Vertical Opening Between Gold Cylinder 1 and Abutment 1 (Average of 3 Measurements)		Vertical Opening Between Gold Cylinder 2 and Abutment 2 (Average of 3 Measurements)	
	Front (μm) $\pm \sigma$	Back (μm) $\pm \sigma$	Front (μm) $\pm \sigma$	Back (μm) $\pm \sigma$
BIR1	210 $\pm$ 10	40 $\pm$ 10	120 $\pm$ 10	30 $\pm$ 20
BIR2	70 $\pm$ 10	40 $\pm$ 10	110 $\pm$ 10	40 $\pm$ 10
COM1	30 $\pm$ 10	20 $\pm$ 10	70 $\pm$ 10	50 $\pm$ 10
COM2	30 $\pm$ 10	190 $\pm$ 10	80 $\pm$ 10	70 $\pm$ 10
COM3	140 $\pm$ 10	120 $\pm$ 10	290 $\pm$ 10	250 $\pm$ 10
GER1	120 $\pm$ 10	100 $\pm$ 10	130 $\pm$ 20	130 $\pm$ 10
GER2	50 $\pm$ 10	20 $\pm$ 10	170 $\pm$ 10	150 $\pm$ 10
GOT1	50 $\pm$ 10	40 $\pm$ 10	160 $\pm$ 10	120 $\pm$ 10
GOT2	10 $\pm$ 10	40 $\pm$ 10	100 $\pm$ 10	30 $\pm$ 10
WAL1	190 $\pm$ 10	120 $\pm$ 10	120 $\pm$ 10	100 $\pm$ 10
WAL2	40 $\pm$ 10	40 $\pm$ 10	140 $\pm$ 10	90 $\pm$ 10

Table 3-3: *In Vitro* **Reference Load**

Superstructure	# of Trials	Abutment 1		Abutment 2	
		Axial Force (N) ±95% Confidence Interval	Bending Moment (N·cm) ±95% Confidence Interval	Axial Force (N) ±95% Confidence Interval	Bending Moment (N·cm) ±95% Confidence Interval
BIR1	20	-300 ± 22	11.9 ± 2.1	-322 ± 19	7.9 ± 1.7
BIR2	20	-294 ± 46	11.0 ± 2.3	-324 ± 55	69.7 ± 4.9
COM1	20	-258 ± 30	10.9 ± 2.4	-250 ± 21	17.9 ± 2.9
COM2	20	-252 ± 35	9.8 ± 1.6	-341 ± 38	16.3 ± 1.8
COM3	20	-233 ± 21	9.4 ± 1.2	-254 ± 51	6.7 ± 3.3
GER1	20	-348 ± 35	21.9 ± 4.2	-342 ± 29	28.2 ± 2.8
GER2	20	-314 ± 16	18.0 ± 2.4	-280 ± 52	19.6 ± 4.7
GOT1	20	-259 ± 27	9.4 ± 1.7	-367 ± 28	3.2 ± 3.1
GOT2	20	-245 ± 37	7.0 ± 2.6	-285 ± 30	3.9 ± 2.1
WAL1	20	-288 ± 27	11.4 ± 2.1	-296 ± 26	3.2 ± 2.6
WAL2	20	-261 ± 54	12.6 ± 1.8	-271 ± 26	5.6 ± 2.1

Table 3-4: *In Vitro* **Resultant Load for Tightening Sequence T1T2**

Superstructure	# of Trials	Abutment 1		Abutment 2	
		Axial Force (N) ±95% Confidence Interval	Bending Moment (N·cm) ±95% Confidence Interval	Axial Force (N) ±95% Confidence Interval	Bending Moment (N·cm) ±95% Confidence Interval
BIR1 (NP)	20	-377 ± 57 *(-77 ±13)*	15.1 ± 2.7 *(3.2 ±0.7)*	-336 ± 25 *(-14 ±7)*	5.4 ± 1.6 *(-2.4 ±0.5)*
BIR2 (P)	20	-254 ± 43 *(40 ±13)*	11.9 ± 7.1 *(-)*	-279 ± 35 *(46 ±14)*	63.4 ± 6.9 *(-6.2 ±1.8)*
COM1 (P)	20	-247 ± 33 *(11 ±9)*	14.3 ± 6.9 *(3.4 ±1.5)*	-184 ± 21 *(67 ±6)*	20.3 ± 4.8 *(2.4 ±1.2)*
COM2 (NP)	20	-242 ± 23 *(-)*	21.4 ± 3.2 *(11.6 ±0.8)*	-283 ± 59 *(58 ±15)*	23.4 ± 8.2 *(7.1 ±1.8)*
COM3 (NP)	20	-310 ± 47 *(-78 ±11)*	33.5 ± 4.2 *(24.0 ±0.9)*	-285 ± 18 *(-31 ±11)*	12.8 ± 1.3 *(6.1 ±0.8)*
GER1 (P)	20	-333 ± 80 *(-)*	31.0 ± 3.0 *(9.0 ±1.1)*	-296 ± 19 *(46 ±7)*	21.7 ± 1.5 *(-6.4 ±0.7)*
GER2 (NP)	20	-351 ± 49 *(-37 ±11)*	45.1 ± 3.8 *(27.1 ±0.9)*	-163 ± 29 *(117 ±12.5)*	30.8 ± 2.9 *(11.2 ±1.2)*
GOT1 (NP)	20	-302 ± 28 *(-43 ±8)*	20.8 ± 1.0 *(11.4 ±0.4)*	-342 ± 34 *(25 ±9)*	3.1 ± 3.0 *(-)*
GOT2 (P)	20	-320 ± 36 *(-75 ±11)*	17.3 ± 5.8 *(10.3 ±1.3)*	-326 ± 40 *(-41 ±10)*	6.7 ± 1.1 *(2.8 ±0.5)*
WAL1 (NP)	20	-281 ± 36 *(-)*	16.3 ± 4.6 *(4.9 ±1.1)*	-296 ± 34 *(-)*	26.0 ± 4.1 *(22.8 ±1.0)*
WAL2 (P)	20	-291 ± 14 *(-29 ±12)*	16.8 ± 0.8 *(4.2 ±0.4)*	-274 ± 21 *(-)*	5.2 ± 2.5 *(-)*

P represents a passive fit and NP represents a non-passive fit. The values in brackets indicate the misalignment load (Resultant − Reference) ±95% confidence interval.

Table 3-5: *In Vitro* **Resultant Load for Tightening Sequence T2T1**

Superstructure	# of Trials	Abutment 1		Abutment 2	
		Axial Force (N) ±95% Confidence Interval	Bending Moment (N·cm) ±95% Confidence Interval	Axial Force (N) ±95% Confidence Interval	Bending Moment (N·cm) ±95% Confidence Interval
BIR1 (NP)	20	-311 ± 17 *(-11 ±6)*	14.8 ± 2.7 *(2.9 ±0.7)*	-362 ± 45 *(-40 ±10)*	4.6 ± 1.8 *(-3.3 ±0.5)*
BIR2 (P)	20	-269 ± 27 *(25 ±11)*	11.3 ± 1.6 *(-)*	-338 ± 77 *(-)*	65.3 ± 10.7 *(-4.4 ±2.5)*
COM1 (P)	20	-312 ± 41 *(-54 ±11)*	10.2 ± 1.1 *(-0.7 ±0.6)*	-227 ± 34 *(24 ±8)*	23.1 ± 4.2 *(5.1 ±1.1)*
COM2 (NP)	20	-240 ± 25 *(12 ±9)*	18.0 ± 1.1 *(8.2 ±0.4)*	-265 ± 17 *(76 ±9)*	23.2 ± 3.4 *(6.9 ±0.8)*
COM3 (NP)	20	-247 ± 34 *(-15 ±8)*	33.9 ± 2.9 *(24.4 ±0.7)*	-268 ± 34 *(-14 ±13)*	12.4 ± 1.4 *(5.6 ±0.8)*
GER1 (P)	20	-292 ± 42 *(56 ±11)*	23.4 ± 2.0 *(1.4 ±1.0)*	-286 ± 24 *(56 ±8)*	21.8 ± 1.2 *(-6.3 ±0.6)*
GER2 (NP)	20	-315 ± 41 *(-)*	38.2 ± 1.5 *(20.2 ±0.6)*	-235 ± 20 *(45 ±12)*	27.7 ± 1.3 *(8.1 ±1.0)*
GOT1 (NP)	20	-300 ± 45 *(-41 ±11)*	22.1 ± 3.6 *(12.7 ±0.8)*	-342 ± 30 *(25 ±9)*	3.1 ± 3.6 *(-)*
GOT2 (P)	20	-315 ± 24 *(-69 ±9)*	13.1 ± 1.9 *(6.0 ±0.7)*	-329 ± 32 *(-44 ±9)*	4.8 ± 3.3 *(0.9 ±0.8)*
WAL1 (NP)	20	-267 ± 21 *(21 ±7)*	23.2 ± 6.5 *(11.9 ±1.4)*	-288 ± 23 *(8 ±7)*	23.5 ± 4.1 *(20.3 ±1.0)*
WAL2 (P)	20	-300 ± 21 *(-39 ±12)*	18.6 ± 2.0 *(6.0 ±0.6)*	-310 ± 23 *(-39 ±7)*	5.1 ± 2.2 *(-)*

P represents a passive fit and NP represents a non-passive fit. The values in brackets indicate the misalignment load (Resultant − Reference) ± 95% confidence interval.

Table 3-6: *In Vitro* Difference in Tightening Sequences (T1T2-T2T1)

Superstructure	Abutment 1		Abutment 2	
	Axial Force (N) ±95% Confidence Interval	Bending Moment (N·cm) ±95% Confidence Interval	Axial Force (N) ±95% Confidence Interval	Bending Moment (N·cm) ±95% Confidence Interval
BIR1	-66 ± 12	(-)	25 ± 11	0.9 ± 0.5
BIR2	15 ± 11	(-)	60 ± 18	(-)
COM1	65 ± 11	4.1 ± 1.5	43 ± 8	-2.8 ± 1.3
COM2	(-)	3.3 ± 0.7	-18 ± 13	(-)
COM3	-63 ± 12	(-)	-18 ± 8	(-)
GER1	-41 ± 19	7.6 ± 0.8	-10 ± 6	(-)
GER2	-36 ± 13	6.9 ± 0.8	72 ± 7	3.1 ± 0.7
GOT1	(-)	-1.3 ± 0.8	(-)	(-)
GOT2	(-)	4.2 ± 1.2	(-)	1.9 ± 0.7
WAL1	-15 ± 9	-6.9 ± 1.7	(-)	2.6 ± 1.2
WAL2	10 ± 5	-1.8 ± 0.5	36 ± 6.5	(-)

Table 3-7: Patient Data

Patient	Male/ Female	Right/Left Auricular Prosthesis	Phase I Surgery	Phase II Surgery	Superstructure Attached	Prosthesis Attached
AB	F	Right	06/26/91	06/26/91	11/06/91	04/12/91
CB	M	Right	11/22/91	03/27/92	09/02/92	09/30/92
HB	F	Left	09/28/94	05/31/95	07/25/95	08/08/95
SF	M	Left	10/27/89	02/16/90	04/04/90	05/09/90

Table 3-8: Patient Abutment Periotest® Values (PTV)

Patient	Abutment 1		Abutment 2	
	PTV	Average$\pm\sigma$	PTV	Average $\pm\sigma$
AB	-6, -5	-5.5±0.7	-5, -5	-5.0±0
CB	-5, -7, -6, -5	-5.8±1.0	-5, -5, -5, -5	-5.0±0
HB	-6, -6, -6, -5	-5.8±0.5	-7, -7, -7	-7.0±0
SF	-6, -6, -5, -6	-5.8±0.5	-5, -5, -5, -5	-5.0±0

Table 3-9: *In Vivo* **Reference Load**

Patient	# of Trials	Abutment 1		Abutment 2	
		Axial Force (N)±σ	Bending Moment (N·cm)±σ	Axial Force (N)±σ	Bending Moment (N·cm)±σ
AB	8	-421±30	17.1±1.4	-260±11	5.0±0.7
CB	8	-434±14	9.5±2.1	-492±40	15.7±1.4
HB	8	-399±54	14.9±1.8	-320±58	8.0±4.4
SF	8	-344±44	14.2±1.7	-310±35	11.5±2.3

Table 3-10: *In Vivo* **Resultant Load Tightening Sequence T1T2**

Patient	# of Trials	Abutment 1		Abutment 2	
		Axial Force (N)±σ	Bending Moment (N·cm)±σ	Axial Force (N)±σ	Bending Moment (N·cm)±σ
AB	6	-440±18 *(-)*	27.2±1.6 *(10.1 ±1.7)*	-259±20 *(-)*	22.8±1.1 *(17.8 ±1.1)*
CB	6	-462±21 *(-27 ±20)*	19.7±2.4 *(10.1 ±2.6)*	-468±47 *(-)*	24.9±3.8 *(9.2 ±3.2)*
HB	6	-443±38 *(-)*	28.0±1.2 *(13.1 ±1.9)*	-194±74 *(126 ±76)*	18.7±2.6 *(11.0 ±4.5)*
SF	6	-355±45 *(-)*	14.6±2.4 *(-)*	-322±66 *(-)*	4.1±2.0 *(-7.0 ±2.6)*

The values in brackets indicate the misalignment load (Resultant – Reference) ±95% confidence interval.

Table 3-11: *In Vivo* **Resultant Load—Tightening Sequence T2T1**

Patient	# of Trials	Abutment 1		Abutment 2	
		Axial Force (N)±σ	Bending Moment (N·cm)±σ	Axial Force (N)±σ	Bending Moment (N·cm)±σ
AB	6	-366 ± 36 *(54 ±38)*	20.9 ± 1.9 *(3.8 ±1.9)*	-212 ± 19 *(48 ±18)*	23.4 ± 1.3 *(18.3 ±1.2)*
CB	6	-424 ± 12 *(-)*	16.6 ± 1.0 *(7.1 ±2.0)*	-426 ± 32 *(66 ±43)*	20.0 ± 0.4 *(4.3 ±1.3)*
HB	6	-355 ± 35 *(-)*	27.7 ± 2.1 *(12.3 ±2.3)*	-192 ± 62 *(129 ±70)*	16.6 ± 1.3 *(8.6 ±4.1)*
SF	6	-344 ± 30 *(-)*	14.7 ± 0.6 *(-)*	-382 ± 11 *(-72 ±32)*	4.8 ± 0.8 *(-6.7 ±2.2)*

The values in brackets indicate the misalignment load (Resultant – Reference) ±95% confidence interval.

Table 3-12: *In Vivo* **Difference in Tightening Sequences (T1T2-T2T1)**

Patient	Abutment 1		Abutment 2	
	Axial Force (N) ±95% Confidence Interval	Bending Moment (N·cm) ±95% Confidence Interval	Axial Force (N) ±95% Confidence Interval	Bending Moment (N·cm) ±95% Confidence Interval
AB	-74 ± 36	6.3 ± 2.3	-46 ± 25	(-)
CB	-37 ± 22	3.1 ± 2.4	(-)	4.9 ± 3.5
HB	-87 ± 47	(-)	(-)	(-)
SF	(-)	(-)	(-)	(-)

Table 3-13: Maximum and Minimum Axial Force During Prosthesis Replacement

Patient	Trial	Abutment 1		Abutment 2	
		Maximum (N)	Minimum (N)	Maximum (N)	Minimum (N)
AB	1	4±14	-13±14	7±14	-13±14
	2	6±18	-14±18	14±17	-3±17
	3	6±17	-10±17	10±16	-6±16
	4	3±17	-20±17	9±15	-6±15
CB	1	19±15	-17±15	13±10	-14±10
	2	7±15	-12±15	15±11	-13±11
	3	4±16	-18±16	9±11	-12±11
	4	6±15	-12±15	13±12	-10±12
HB	1	23±17	-16±17	16±12	-17±12
	2	23±12	-4±12	14±13	-9±13
	3	11±15	-15±15	5±13	-26±13
	4	26±14	-3±14	9±12	-23±12
SF	1	6±32	-21±32	5±22	-25±22
	2	7±15	-25±15	11±13	-23±13
	3	14±14	-39±14	25±11	-51±11
	4	7±13	-22±13	14±11	-19±11

Table 3-14: Maximum Bending Moment During Prosthesis Replacement

Patient	Trial	Abutment 1 Maximum Bending Moment (N·cm)	Abutment 2 Maximum Bending Moment (N·cm)
AB	1	7.2±0.6	13.0±0.6
	2	8.8±0.7	6.5±0.7
	3	8.0±0.7	6.7±0.5
	4	8.3±0.6	8.0±0.7
CB	1	4.0±0.8	4.4±0.3
	2	3.6±0.5	9.5±0.6
	3	2.9±0.8	11.4±0.4
	4	2.8±0.7	10.7±0.6
HB	1	5.4±0.6	6.4±0.5
	2	3.6±0.5	4.7±0.7
	3	10.9±0.6	9.1±0.4
	4	5.7±0.6	9.7±0.7
SF	1	6.4±0.5	22.1±1.1
	2	6.3±0.5	13.9±0.6
	3	13.0±0.6	37.3±0.4
	4	4.2±0.6	15.5±0.4

Table 3-15: Maximum and Minimum Axial Force During Prosthesis Removal

Patient	Trial	Abutment 1		Abutment 2	
		Maximum (N)	Minimum (N)	Maximum (N)	Minimum (N)
AB	1	9±17	-2±17	21±17	-1±17
	2	7±18	-6±18	28±16	0±16
	3	4±19	-11±19	22±16	-1±16
	4	10±19	-1±19	30±17	0±17
CB	1	12±16	-4±16	4±11	-14±11
	2	14±16	-2±16	6±11	-12±11
	3	14±16	-2±16	7±10	-10±10
	4	9±15	-3±15	7±12	-7±12
HB	1	24±13	-3±13	20±13	0±13
	2	18±15	-2±15	24±12	0±12
	3	25±16	-2±16	20±13	0±13
	4	28±14	-4±14	15±12	0±12
SF	1	11±29	-3±29	14±22	-1±22
	2	11±18	-3±18	24±13	-2±13
	3	13±17	-3±17	5±12	-4±12
	4	12±16	-1±16	13±14	-1±14

Table 3-16: Maximum Bending Moment During Removal of Prosthesis

Patient	Trial	Abutment 1 Maximum Bending Moment (N·cm)	Abutment 2 Maximum Bending Moment (N·cm)
AB	1	11.9±0.8	18.6±0.5
	2	14.2±0.6	20.5±0.7
	3	16.3±0.6	17.0±0.3
	4	15.2±0.7	19.1±0.4
CB	1	8.9±0.9	11.1±0.5
	2	7.6±0.7	9.4±0.7
	3	7.2±1.0	8.7±0.3
	4	6.2±0.8	6.8±0.5
HB	1	3.9±0.5	4.5±0.6
	2	3.4±0.7	4.1±0.8
	3	4.4±0.5	5.8±0.6
	4	4.5±0.6	4.4±0.6
SF	1	13.0±0.8	10.2±1.0
	2	10.9±0.6	6.4±0.8
	3	16.5±0.6	13.5±0.7
	4	12.0±0.5	6.2±0.8

Table 3-17: Coordinates of Implants and Activation Points For Superstructure Model

	x-coordinate (mm)	y-coordinate (mm)
Implant 1	0	-10.35
Implant 2	0	10.35
Activation point 1	4.7	-14.3
Activation point 2	0	0
Activation point 3	5.3	13.4

Table 3-18: Magnitude of Applied Forces for Model Input

	Case 1	Case 2	Case 3
Activation Point 1	6.7N	20N	20N
Activation Point 2	6.7N	-40N	-20N
Activation Point 3	6.7N	20N	20N
Axial Force	20N	0	20N
Bending Moment	6.7N·cm	20N·cm	20N·cm

Table 3-19: Force Predictions on Implants 1 and 2 using the Skalak and BH Models

Case	Skalak		BH			
	Implant 1 (N)	Implant 2 (N)	Implant 1 Axial Force (N)	Implant 1 Bending Moment (N·cm)	Implant 2 Axial Force (N)	Implant 2 Bending Moment (N·cm)
1	10.3	9.7	10.3	3.3	9.7	3.3
2	0.9	-0.9	0.8	10.0	-0.8	10.0
3	10.9	9.1	10.8	10.0	9.2	10.0
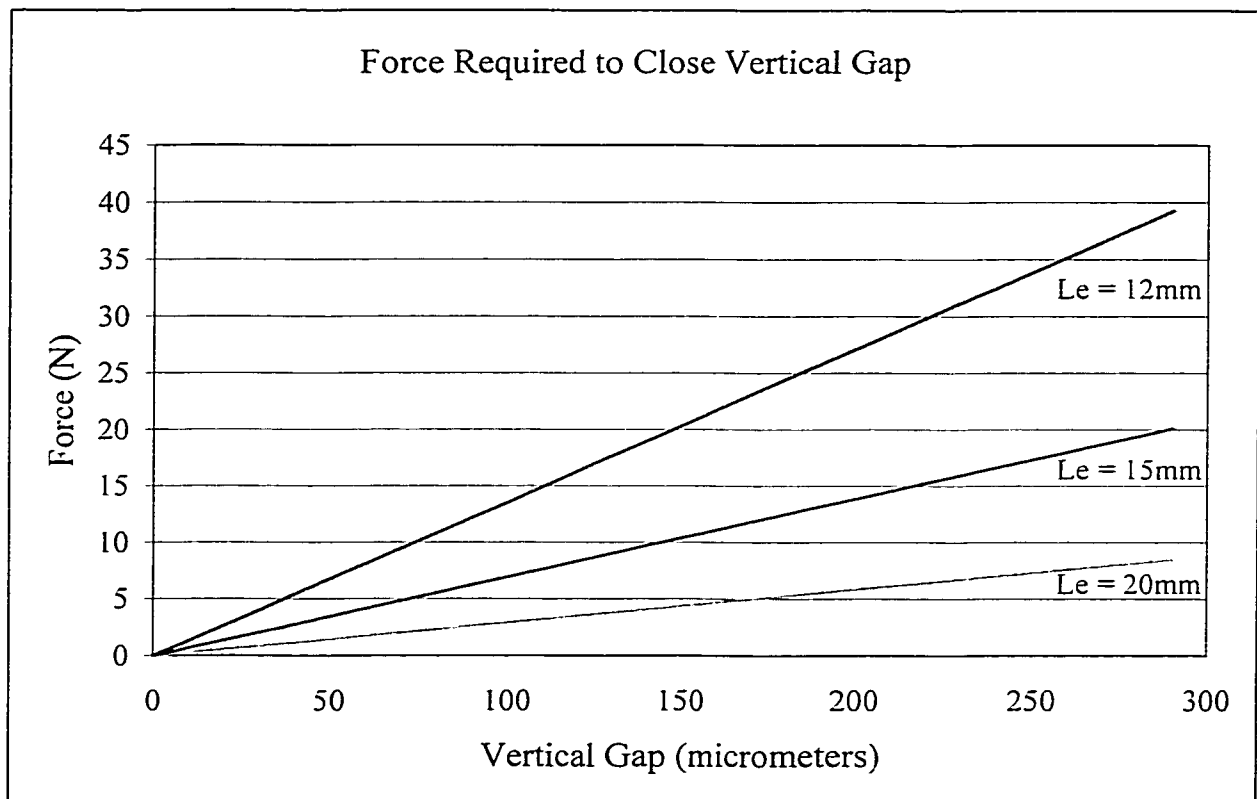
Figure 3-1: Theoretical Force Required to Close Gap

In Vitro T1T2 Resultant Axial Force
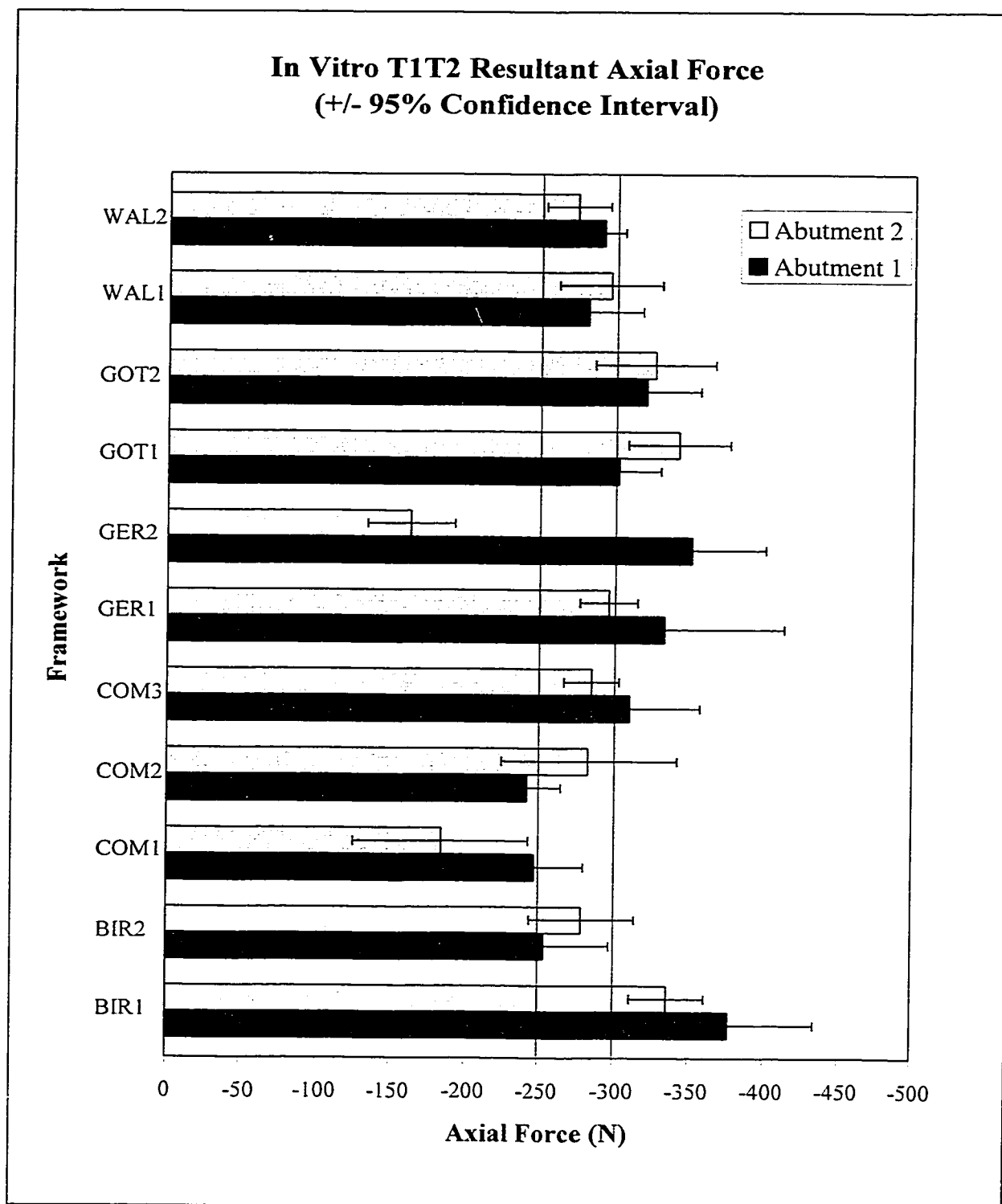**(+/- 95% Confidence Interval)**

Figure 3-2: Comparison of T1T2 Resultant Axial Force and Optimum Preload
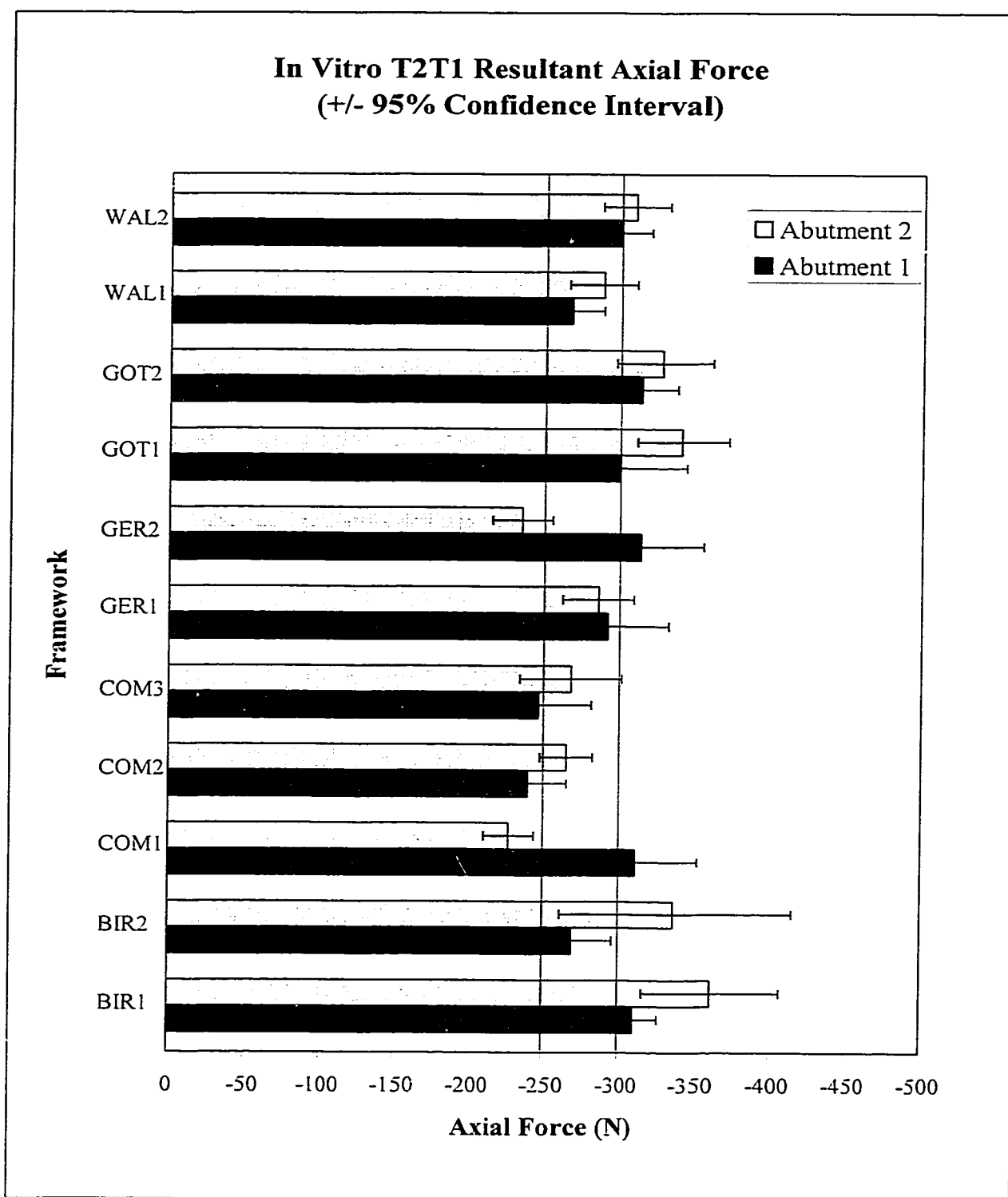
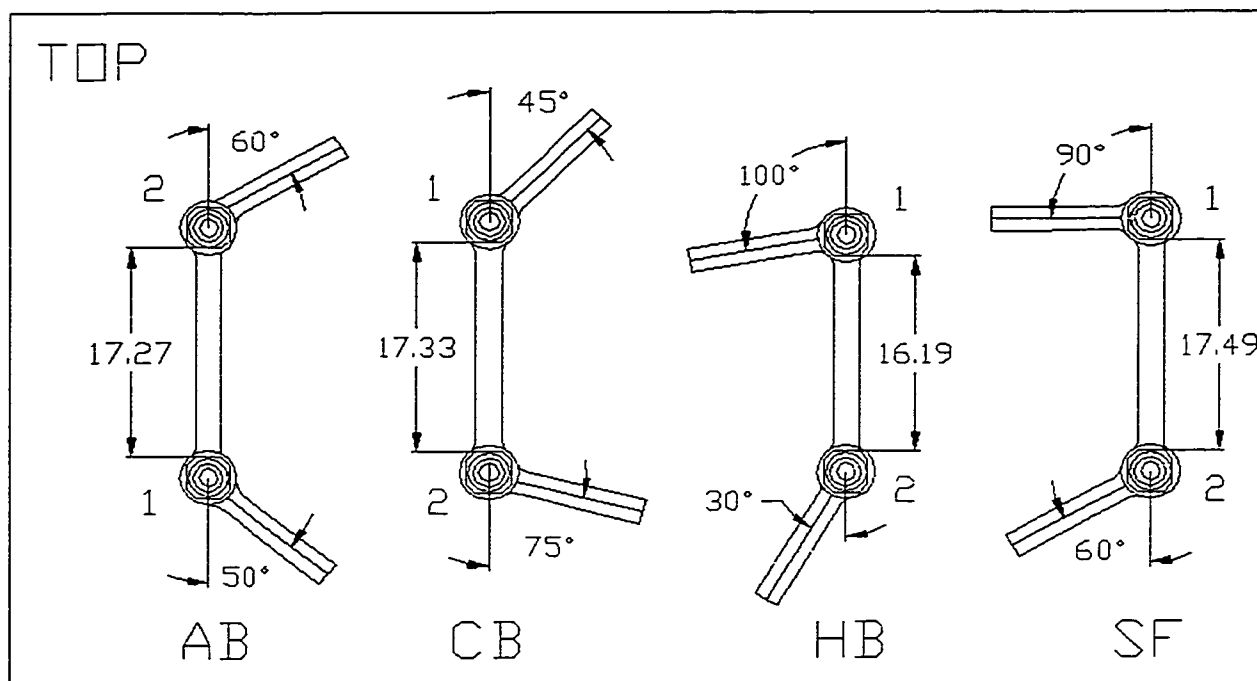**Figure 3-3: Comparison of T2T1 Resultant Force and Optimum Load**

Figure 3-4: *In Vivo* **Superstructures (Dimensions are in mm)**
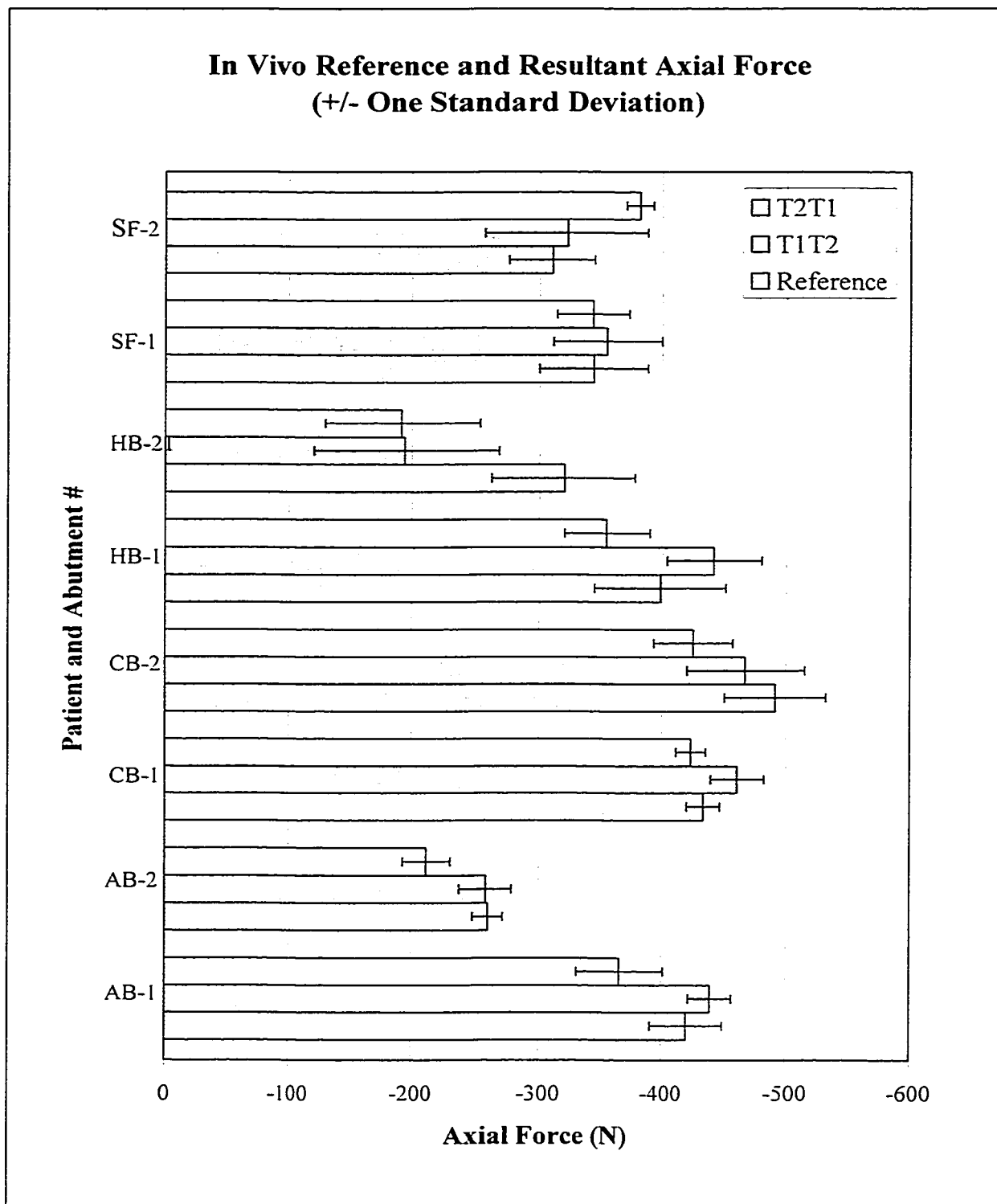
Figure 3-5: Comparison of *In Vivo* Reference and Resultant Axial Force
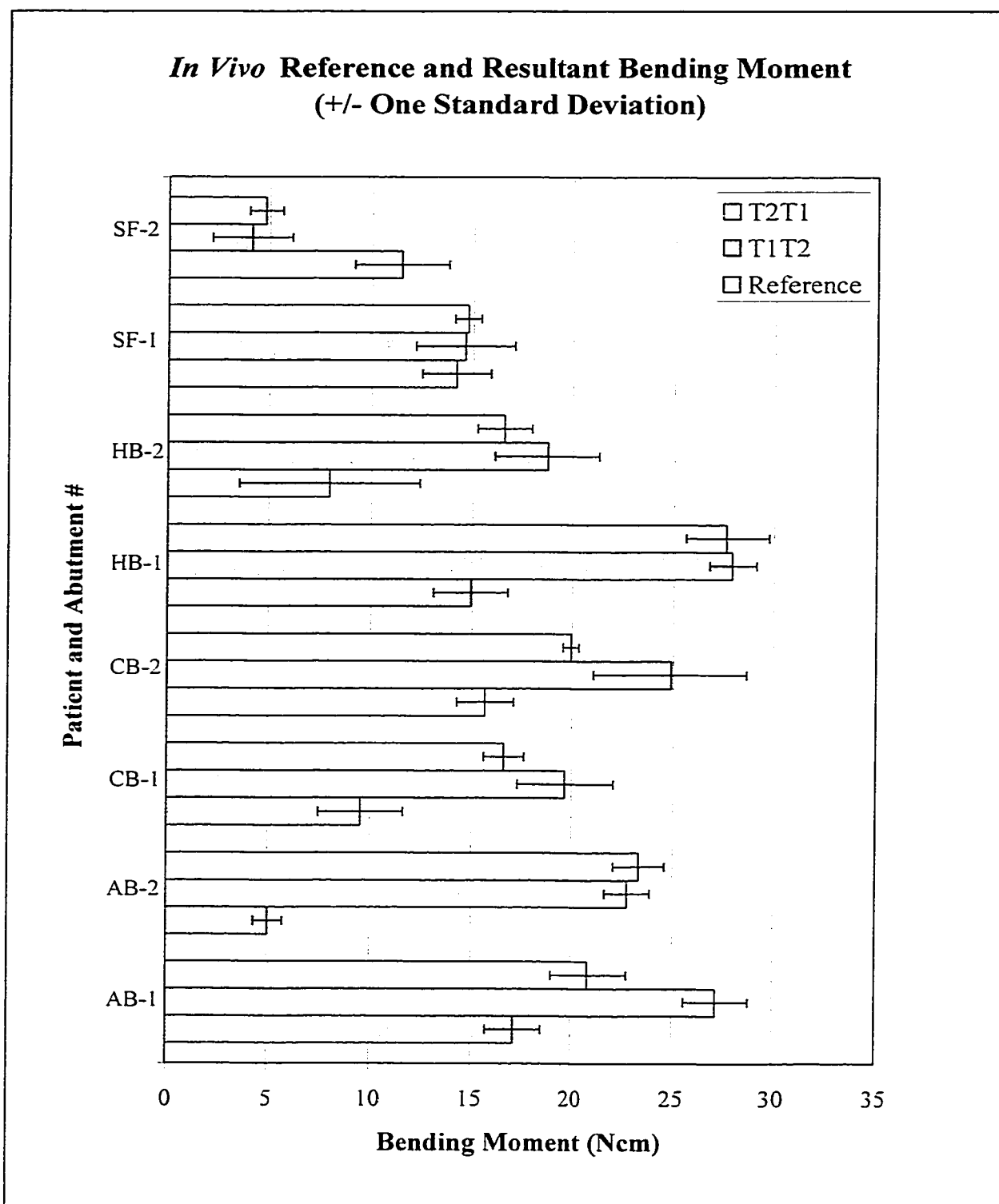
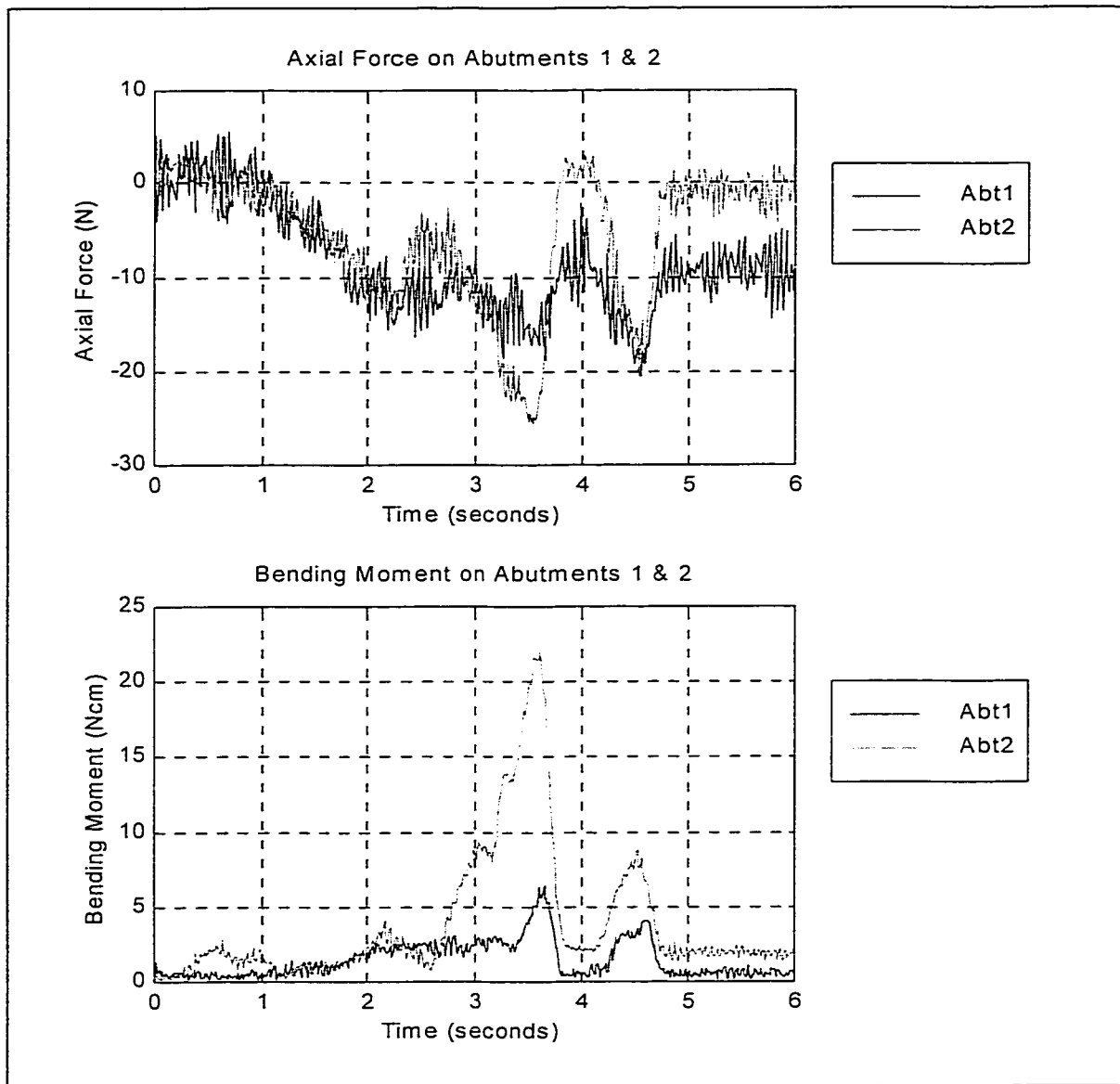Figure 3-6: Comparison of *In Vivo* Reference and Resultant Bending Moment

Figure 3-7: Prosthesis Replacement 1-Patient SF

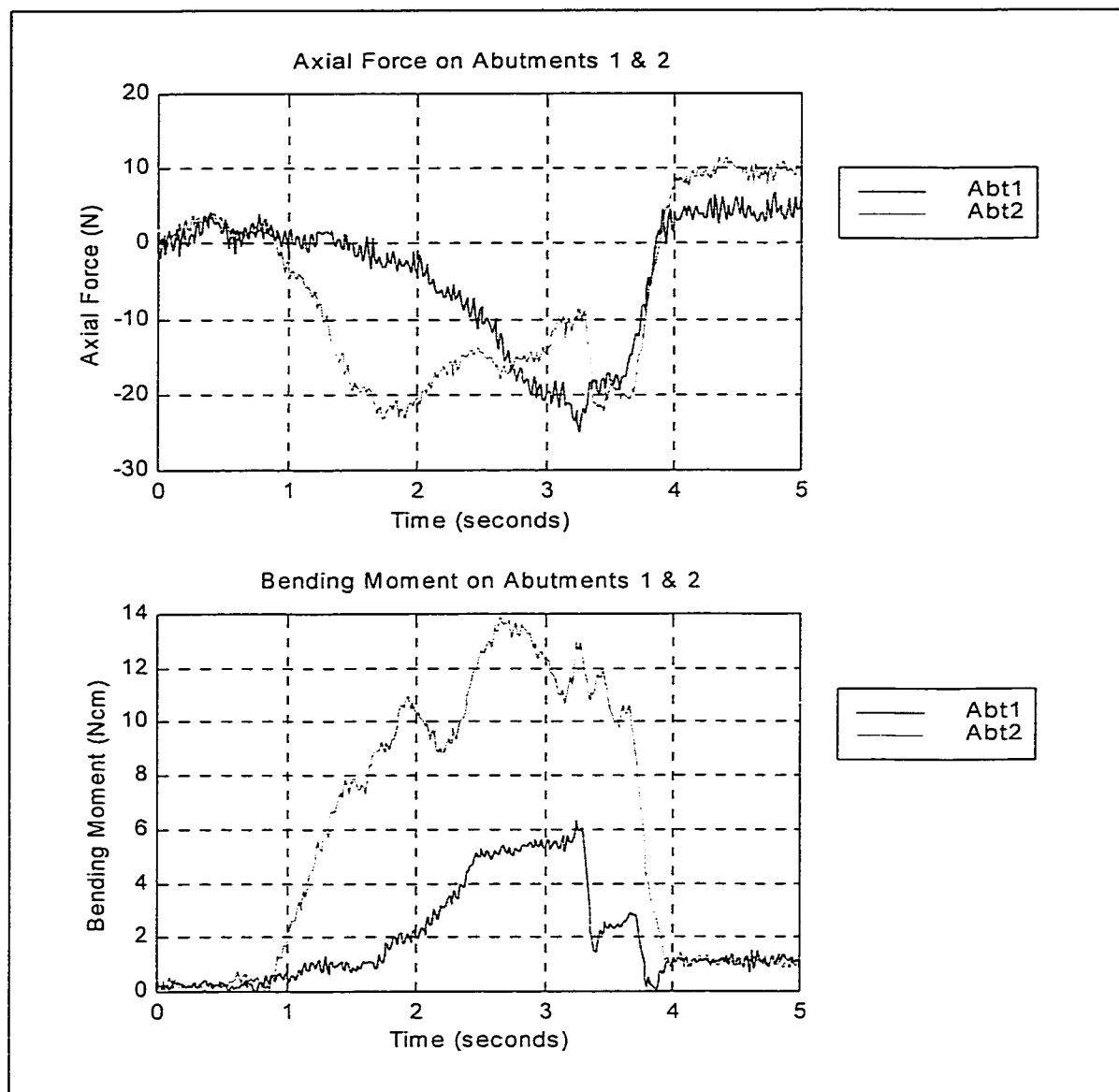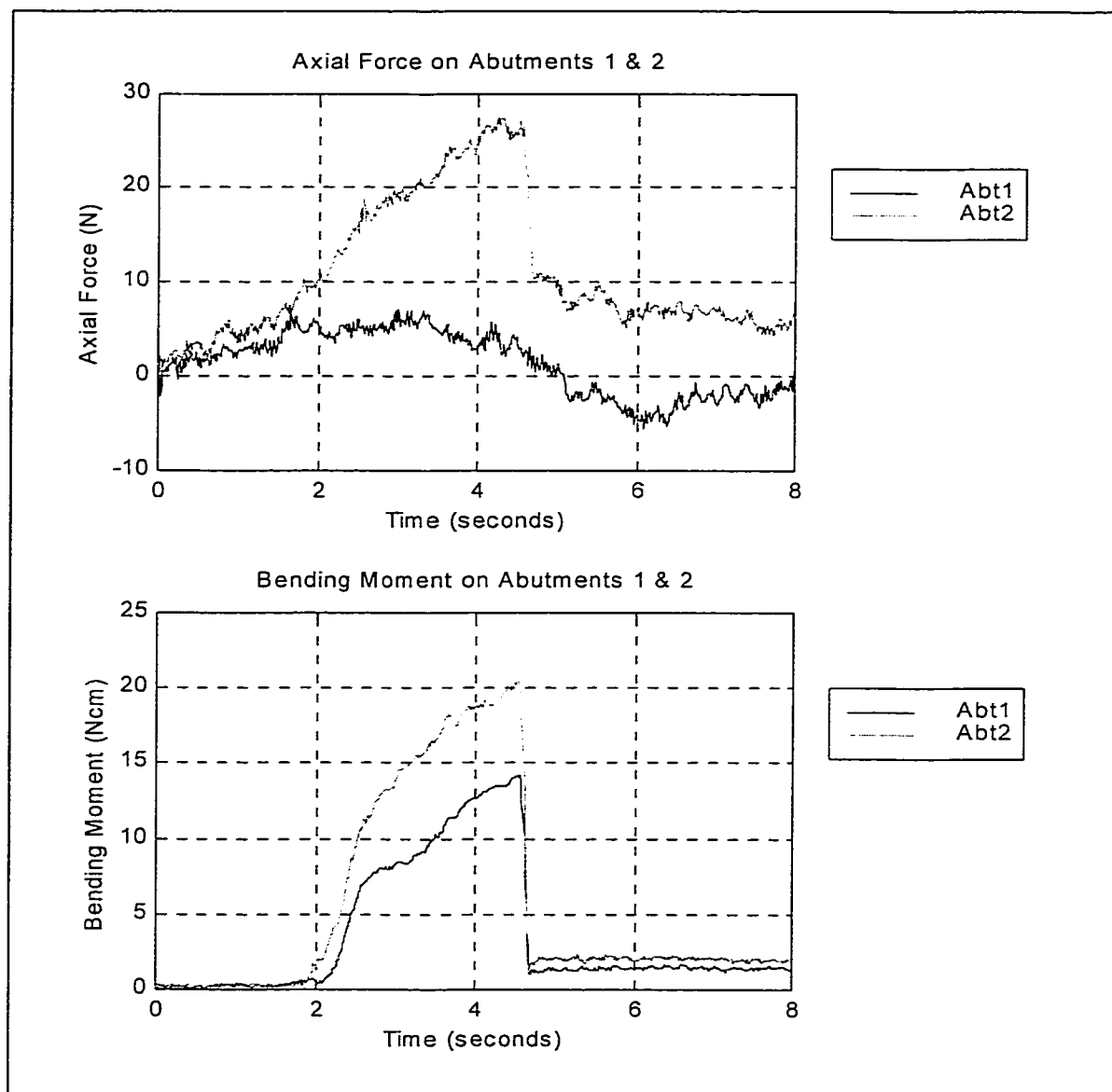**Figure 3-8: Prosthesis Replacement 2-Patient SF**

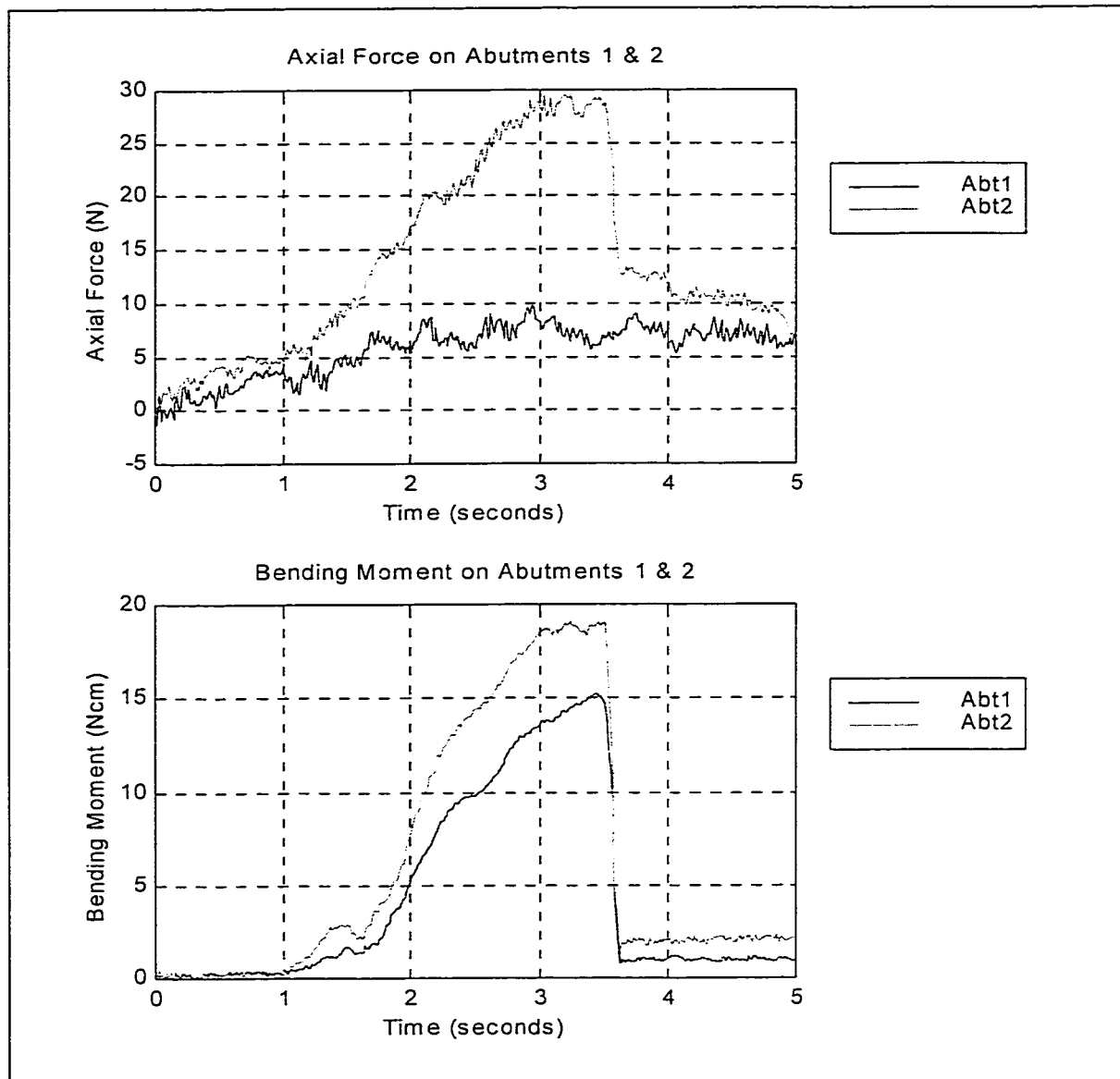**Figure 3-9: Prosthesis Removal 2-Patient AB**
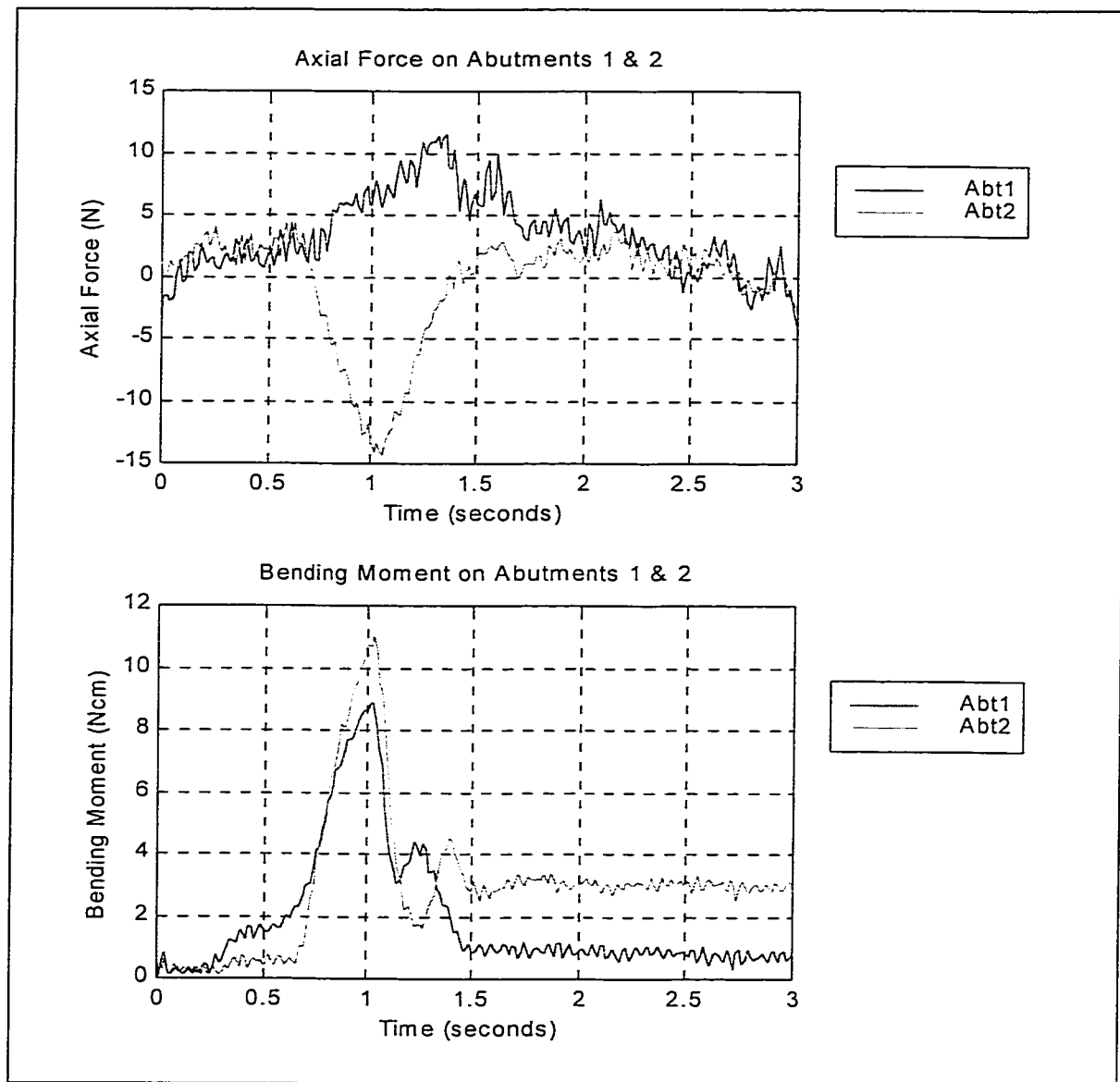
Figure 3-10: Prosthesis Removal 4-Patient AB

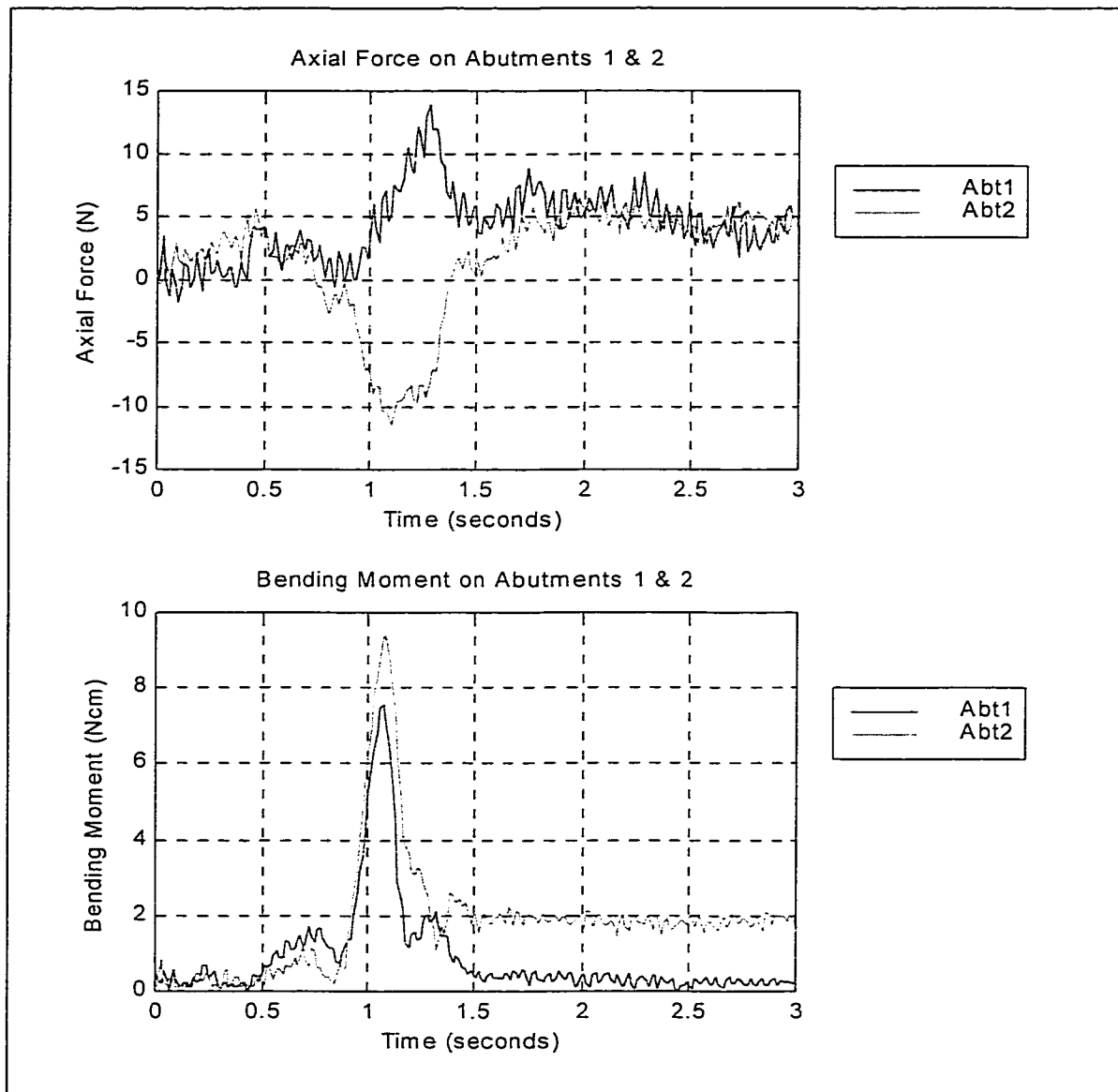**Figure 3-11: Prosthesis Removal 1-Patient CB**

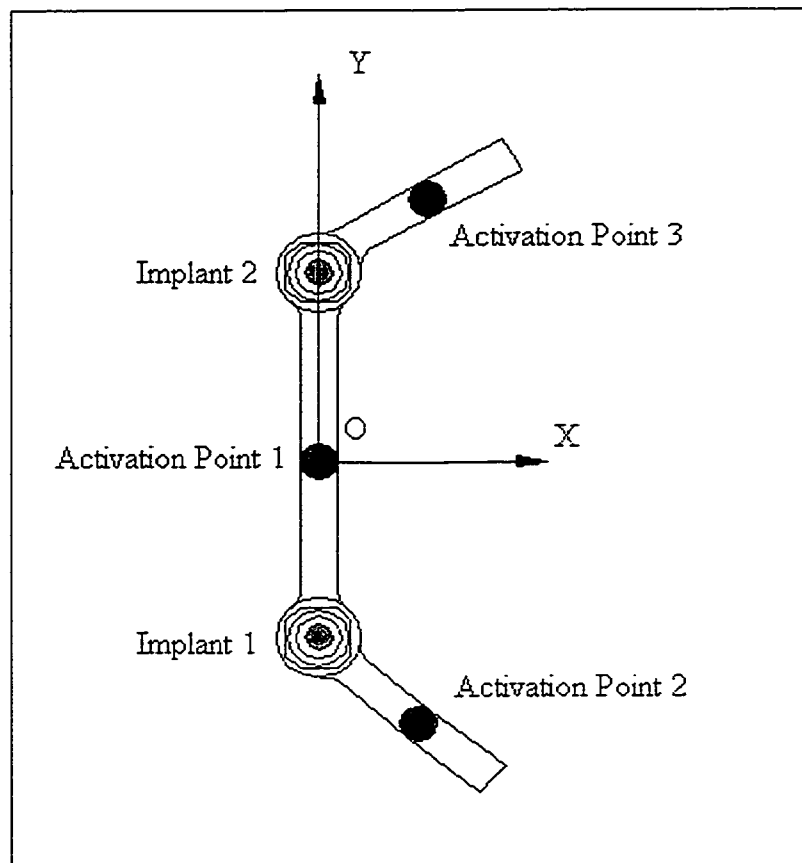**Figure 3-12: Prosthesis Removal 2-Patient CB**

Figure 3-13: Superstructure Model Used for Force Predictions

Chapter 4

Conclusions

The purpose of this study was to determine the character and magnitudes of loads generated on craniofacial implants, including how superstructure misfit affected preload, and whether various biomechanical models developed for oral implants can be used to predict the loading of craniofacial implants. To investigate this, load and misfit measurements were made both *in vitro* and *in vivo*.

In the *in vitro* study there were eleven superstructures evaluated. The superstructures were all constructed for the same implant configuration, but by five different craniofacial prosthetic centers in the world. The vertical misfit for the superstructures was measured with a cathetometer. Five out of eleven superstructures were considered to have a passive fit as defined by the work of Jemt (1991). Jemt indicated that for intraoral implants a misfit of 150µm, as determined by the screw resistance tests, was clinically acceptable. Most of the measured vertical gaps varied from front to back indicating that there was rotational misfit as well. The average reference load measured was −290N,

which was within the optimum preload range of –250N to –300N. There was no correlation between the magnitude of vertical misfit and misfit load. Some of the superstructures that were considered passive had misfit loads as large as those in the non-passive superstructures. This can be attributed to the fact that horizontal misfit and rotational misfit are not accounted for with the one-screw test, as well as variations in applied torque. All these could have a significant effect on the misfit load. All of the superstructures showed a significant difference between the resultant loads for the two tightening sequences.

Four patients participated in the *in vivo* study that was done at the COMPRU at the Misericordia Hospital in Edmonton, Alberta. The superstructures were first clinically assessed for misfit using the one-screw test, and then the preload and functional load were measured. According the clinical one-screw test, all of the superstructures were considered to have a passive fit. The average reference value measured for the *in vivo* tests was –373N, which is higher than both the measured *in vitro* reference load and the optimum preload range. However, due to electrical noise in the *in vivo* testing there was significant error in the measurements. Although all of the superstructures were considered to be passive, all of the superstructures had significant misfit load. Once again, the vertical misfit cannot account for horizontal or rotational misfits. Additionally, there was a significant difference between the two tightening sequences for three out of four patients. The differences in tightening sequence should be taken in light of the fact that the 95% confidence intervals for the difference in means were high, up to 59% of the actual value.

The functional loads for replacement and removal of the prosthesis were measured for each superstructure. Each replacement trial had a unique profile that was dependent upon the order that the clips were engaged. The axial force varied from –51N to 26N and the bending moments varied from 2.8N·cm to 37.3N·cm. The removal trials showed more consistency for each patient. The average force required to remove the prosthesis was 24N which slightly higher than the removal forces measured by Del Valle (1995) of 15N to 23N. The moment loads varied from 3.4N·cm to 20.5N·cm and the bending moment on each abutment followed similar profiles, but with different magnitudes. This could indicate that there is a stiffness difference between the two implant sites.

An evaluation of the Skalak model and the Brunski and Hurley (BH) model was done using the superstructure of patient AB. Since Skalak's model does not allow bending moments on the implants, there is little correlation between the predicted values and those measured *in vivo*. The BH model, when both implants had the same axial and bending stiffness, also did not predict values similar to those measured. However, if the stiffnesses were varied the BH model could predict values close to those measured.

From these results the following conclusions were made:

- The one-screw test is not a good measure of passivity, since it does not account for horizontal and rotational misfits.

- The clinically acceptable vertical misfit of 150μm does not have a direct correlation with the measured misfit loads.

- The implant site axial and bending stiffnesses can vary significantly between craniofacial sites.

- The BH model could be a useful tool in predicting the loading on craniofacial implants, if the axial and bending stiffnesses of the implants are known.

- There was no difference found between the superstructure construction technique (i.e. flame soldered or laser welded) and the misfit of the superstructure.

REFERENCES

[1] Brånemark, P., Zarb, G.A., Alberktsson, T. *Tissue-Integrated Prostheses Osseointegration in Clinical Dentistry.* Quintessence Publishing Co., Inc 1985.

[2] Brunski, J.B. "Biomechanical Factors Affecting the Bone—Dental Implant Interface." *Clinical Materials,* Volume 10, Pages 153-201, 1992.

[3] Brunski, J.B., Skalak, R. "Biomechanical Considerations for Craniofacial Implants." *Osseointegration in Craniofacial Reconstruction,* Edited by P-I Brånemark and Dan E. Tolman, Quintessence Publishing Co., Inc., Carol Stream, IL, 1998.

[4] Burguete, R.L., Johns, R.B., King, T., Patterson, E.A. "Tightening characteristics for screwed joints in osseointegrated dental implants." *Journal of Prosthetic Dentistry,* Volume 71, Pages 592-599, 1994.

[5] Dally, J.W., Riley, W.F., McConnell, K.G. *Instumentation for Engineering Measurements.* John Wiley & Sons, Inc., 1984.

[6] Del Valle, V.R. *Loading and Strain Distribution from Osseointegrated Craniofacial Implants.* M.Sc. Thesis, University of Alberta, Edmonton, Alberta, 1995.

[7] Faulkner, M.G., Berg, K.L. "Biomechanical Implications for Craniofacial Osseointegration." Ear Reconstruction/98, Banff National Park, March 4-6, 1998.

[8] Frost, H.M. "The mechanostat: a proposed pathogenic mechanism of osteoporoses and the bone mass effects of mechanical and nonmechanical agents." *Bone and Mineral,* Volume 2, Pages 73-85, 1987.

[9]   Glantz, P.O., Rangert B., Svensson, A., Stafford, G.D., Arnvidarson, B., Randow, K., Linden, U., Hultén, J. "On clinical loading of osseointegrated implants: A methodological and clinical study." *Clinical Oral Implants Research*, Volume 4, Pages 99-105, 1993.

[10]   Jemt, T. "Failures and Complications in 391 Consecutively Inserted Fixed Prostheses Supported by Brånemark Implants in Edentulous Jaws: A Study of Treatment From the Time of Prosthesis Placement to the First Annual Checkup." *International Journal of Oral and Maxillofacial Implants*, Volume 6, Pages 270-276, 1991.

[11]   May, K.B., Edge, M.J. Russell, M.M., Razzoog, M. E., Lang, B. R. "The precision of fit at the implant prosthodontic interface." *Journal of Prosthetic Dentistry*, Volume 77, Number 5, Pages 497-502, 1997.

[12]   Meredith, N., Friberg, B., Sennerby, L. Aparicio, C. "Relationship Between Contact Time Measurements and PTV Values When Using the Periotest to measure Implant Stability." *International Journal of Prosthodontics*, Volume 11, Pages 269-275, 1998.

[13]   Morgan, M.J., James, D.F. "Force and Moment Distributions Among Osseointegrated Dental Implants." *Journal of Biomechanics*, Volume 28, Number 9, Pages 1103-1109, 1995.

[14]   Rangert, B., Gunne, J. "Mechanical Aspects of a Brånemark Implant Connected to a Natural Tooth: An In Vitro Study" *International Journal of Oral and Maxillofacial Implants*, Volume 6, Pages 177-186, 1991.

[15]   Skalak, R. "Biomechanical considerations in osseointegrated prostheses." *Journal of Prosthetic Dentistry*, Volume 49, Number 6, Pages 843-848, 1983.

[16] Smedberg, J.I., Nilner, K., Rangert, B., Svensson, S.A., Glantz, P.O. "On the influence of superstructure connection on implant preload: A methodological and clinical study." Clinical Oral Implants Research, Volume 7, Pages 55-63, 1996.

[17] Taylor, T.D., Agar, J.R., Vogiatzi, T. "Implant Prosthodontics: Current Perspective and Future Directions." *International Journal of Oral and Maxillofacial Implants*, Volume 15, Pages 66-75, 2000.

Appendix A

Component Dimensions

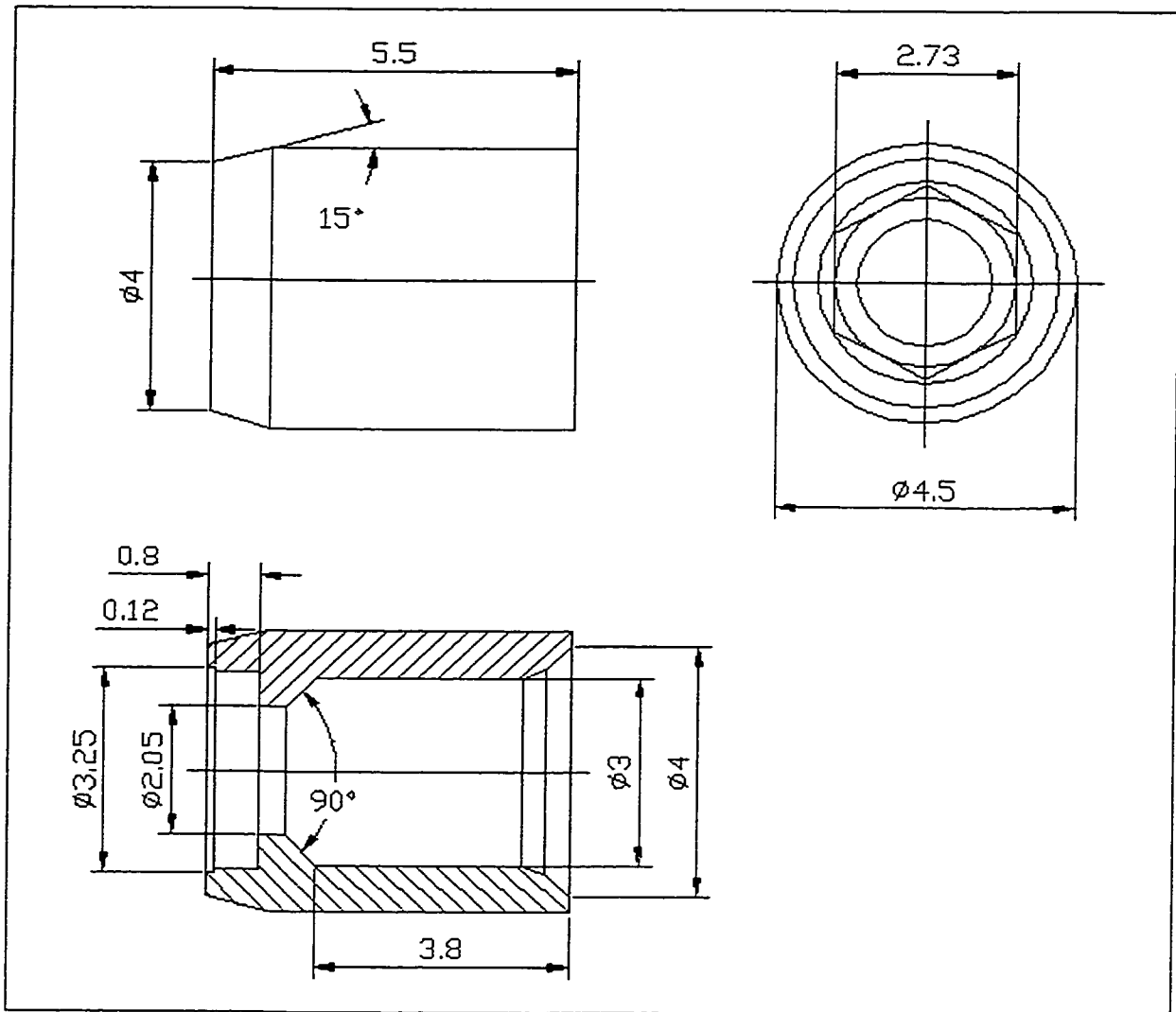**Figure A-1: Nobel Biocare 4mm Flanged Fixture (All dimensions in mm)**

Figure A-2: Nobel Biocare 5.5mm Abutment (All dimensions in mm)

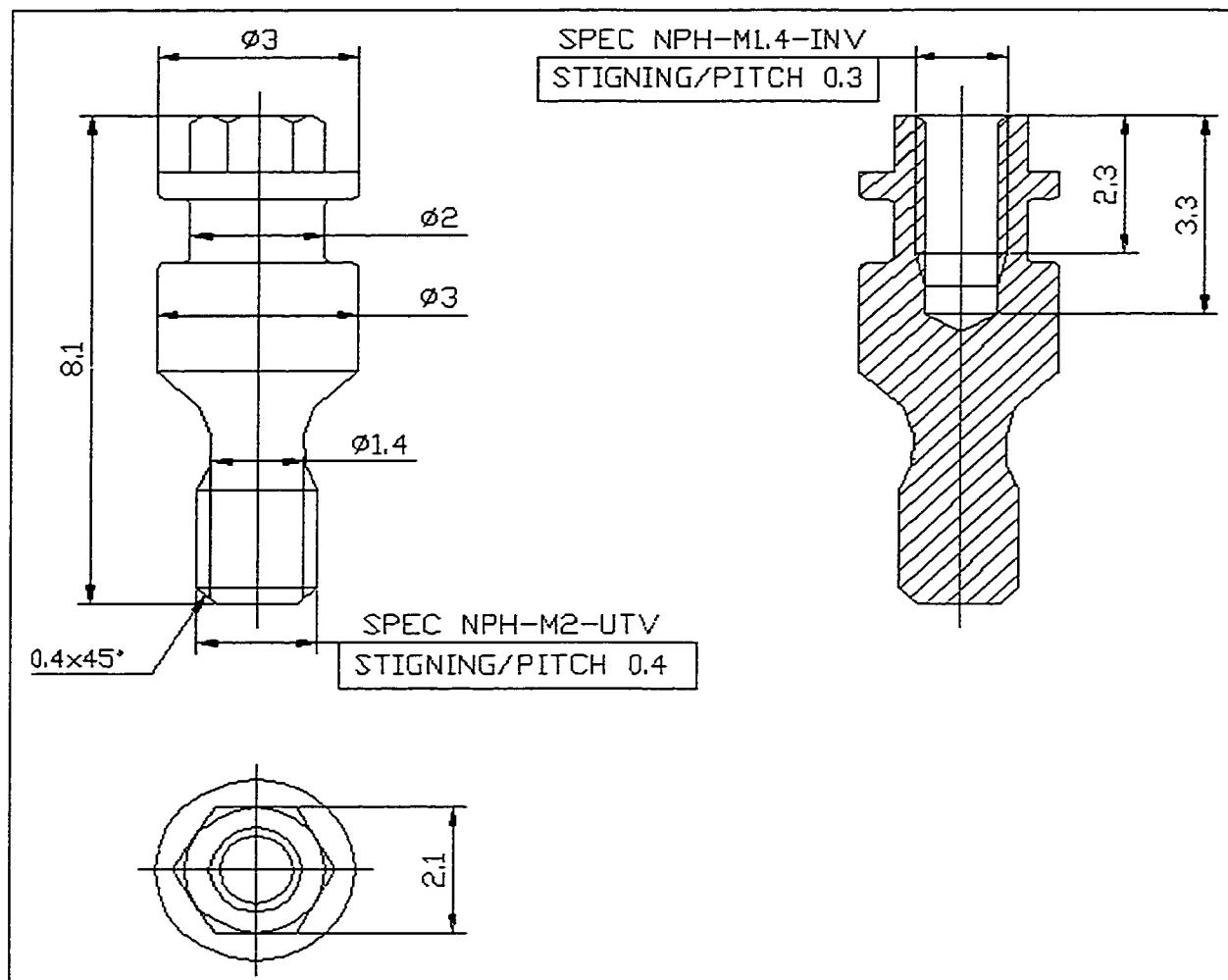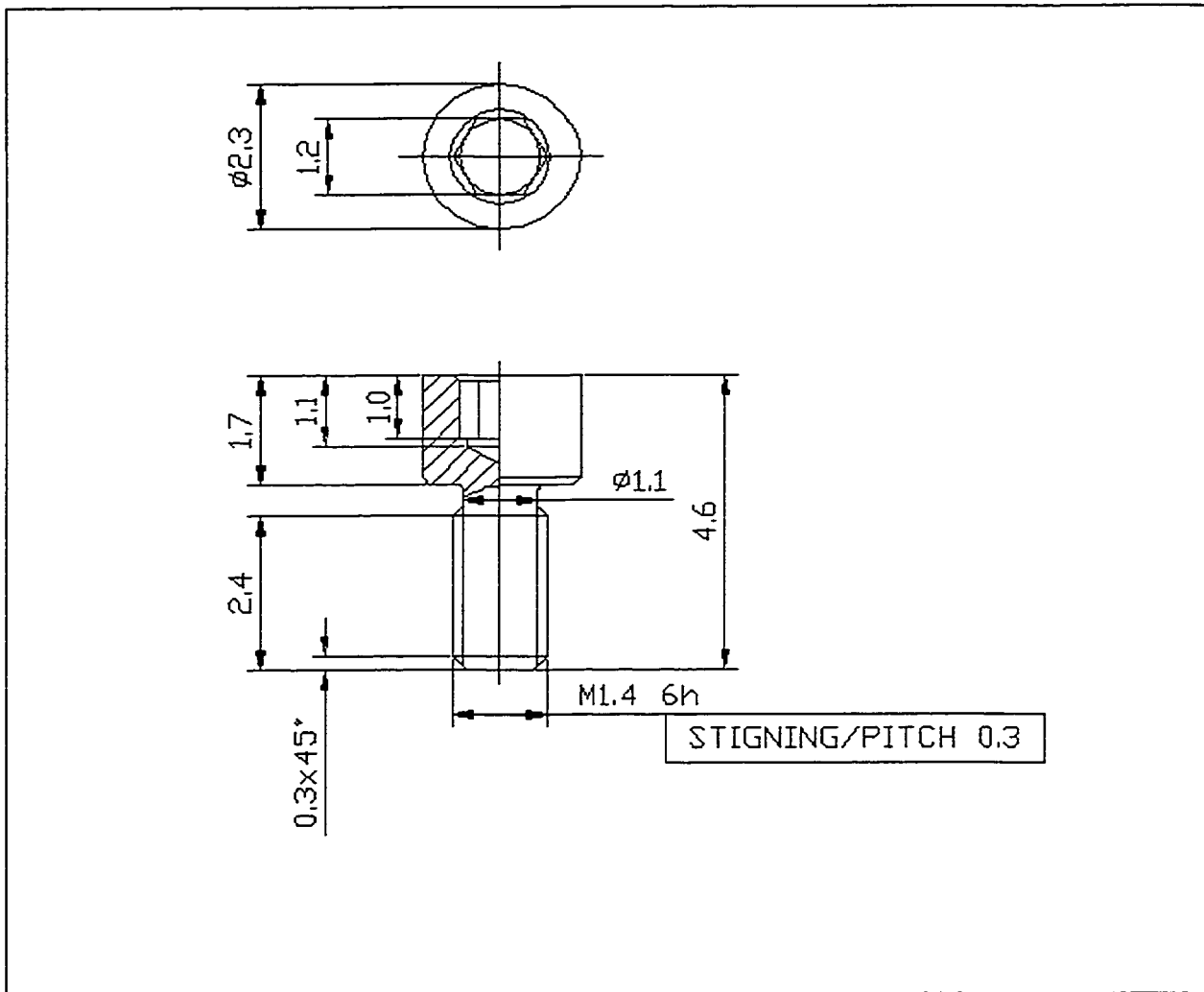**Figure A-3: Nobel Biocare 5.5mm Abutment Screw (All dimensions in mm)**

Figure A-4: Nobel Biocare Hexagon Head Gold Screw (All dimensions in mm)
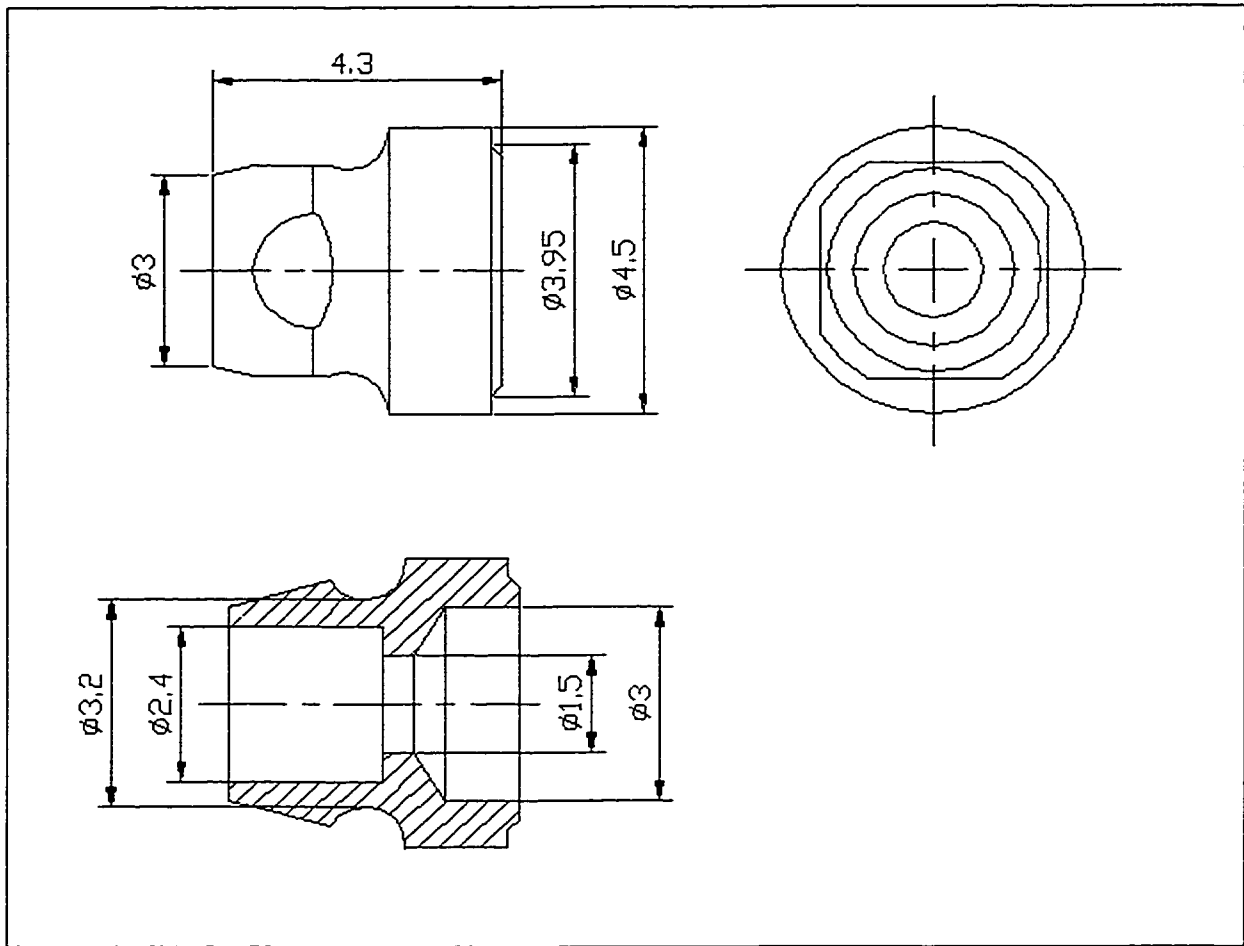
Figure A-5: Nobel Biocare 4mm Gold Cylinder (All dimensions in mm)
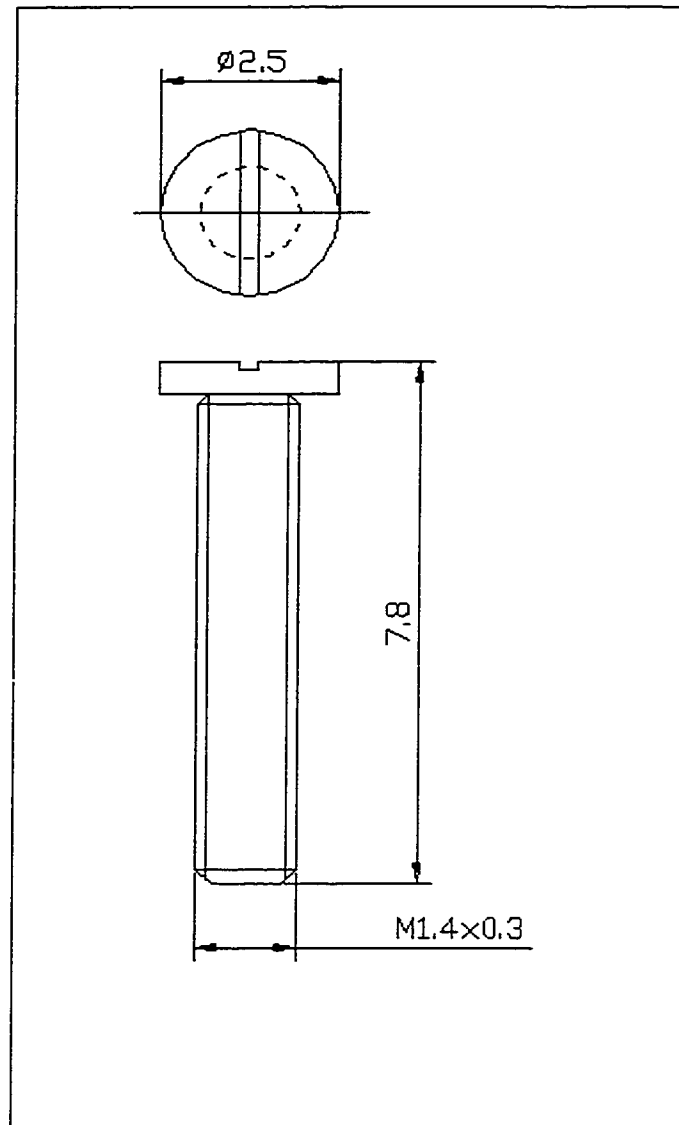
Figure A-6: Calibration Screw (All dimensions in mm)

Appendix B

Calibration Theory

This appendix outlines the calibration procedure used. If a force is applied at a distance perpendicular to gauge there the strain produced is a combination of the strain caused by the axial force and the strain caused by the bending moment, see Figure B-1.

The strain caused by the axial force is

$$\varepsilon = \frac{F}{AE} \qquad \textbf{(B-1)}$$

where A is the cross-section area of the abutment and E is the modulus of elasticity.

The strain caused by the bending moment is

$$\varepsilon = \frac{My}{EI} \qquad \textbf{(B-2)}$$

where y is the distance between the force and the strain gauge and I is the moment of inertia.

Therefore the strain experienced by the strain gauge is

$$\varepsilon = \frac{F}{AE} + \frac{My}{EI}$$
(B-3)

For a linear strain gauge the voltage reading in μV can be converted to strain by

$$\varepsilon = \frac{G}{K_g}$$
(B-4)

where K_g is the gauge factor and G is the gauge reading in μV.

Combining equation (B-3) and equation (B-4),

$$G = \frac{K_g F}{AE} + \frac{K_g My}{EI}.$$
(B-5)

If the force was not applied perpendicular to the gauge, the strain experienced by the

gauge would be a combination of the axial force and the component of the moment

perpendicular to the gauge. If the moment is broken in to the moment about the x-axis

and the moment about the y-axis the resulting strain would be

$$G = \frac{K_g F}{AE} + \frac{K_g M_x y}{EI} \sin\theta + \frac{K_g M_y y}{EI} \cos\theta$$
(B-6)

where θ is the angle between the x-axis and the gauge of interest.

The study abutment used had three strain gauges with an angle of approximately 120°

between gauges. For calibration purposes gauge 1 was placed approximately on the y-

axis as shown in Figure B-2. Since the strain gauges covered a relatively large area of the

abutment and the gauges were small and difficult to install on the equally small abutment

it was hard to identify the exact location and orientation of the strain gauges. As a result

the values of K_g, A, I, and y are unknown but are constants. If the constants are

combined, equation   (B-6) can be represented by the following multiple regression equation

$$G = a + bF + cM_x + dM_y \qquad \text{(B-7)}$$

where a, b, c, and d are regression coefficients.

During the calibration, the force, distance, and angle between the x-axis and the line from the applied force to the center of the abutment were varied and the three gauge readings were recorded. The applied force, distance, and angle were used to calculate F, M_x, and M_y. The regression coefficients could then be determined by using the method of least squares, which minimizes the error between the actual gauge reading and the calculated gauge reading. The set of equations used to determine the regression coefficients are ginve by Dally et al. 1984.

The resulting equations for gauges 1, 2, and 3 for abutment 1 are:

$$G_1 = 0.48 - 0.59F - 0.90M_x - 0.11M_y \qquad \text{(B-8)}$$

$$G_2 = -0.43 - 1.1F + 0.54M_x - 0.70M_y \qquad \text{(B-9)}$$

$$G_3 = 1.11 - 0.54F + 0.37M_x - 0.82M_y \qquad \text{(B-10)}$$

The correlation coefficients are 0.988, 0.985, 0.995 for gauges 1, 2, and 3.

The resulting equations and correlation coefficients for gauges 1, 2, and 3 for abutment 2 are:

$$G_1 = 0.66 - 0.70F - 0.70M_x - 0.06M_y \qquad \text{(B-11)}$$

$$G_2 = 1.90 - 0.73F + 0.33M_x - 0.88M_y \qquad \textbf{(B-12)}$$

$$G_3 = 2.15 - 1.06F + 0.41M_x + 0.77M_y \qquad \textbf{(B-13)}$$

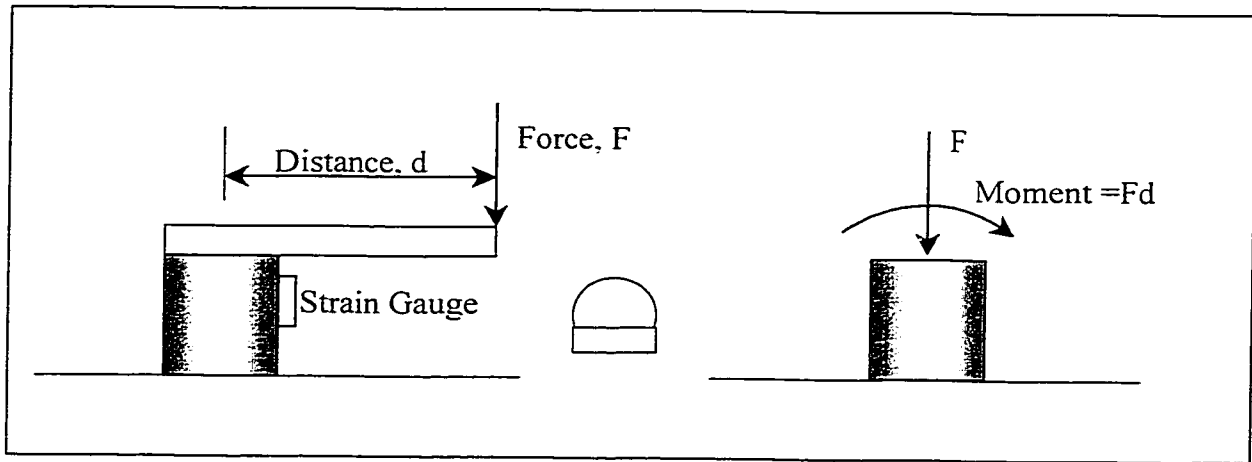The correlation coefficients are 0.985, 0.991, and 0.993 for gauges 1, 2, and 3.

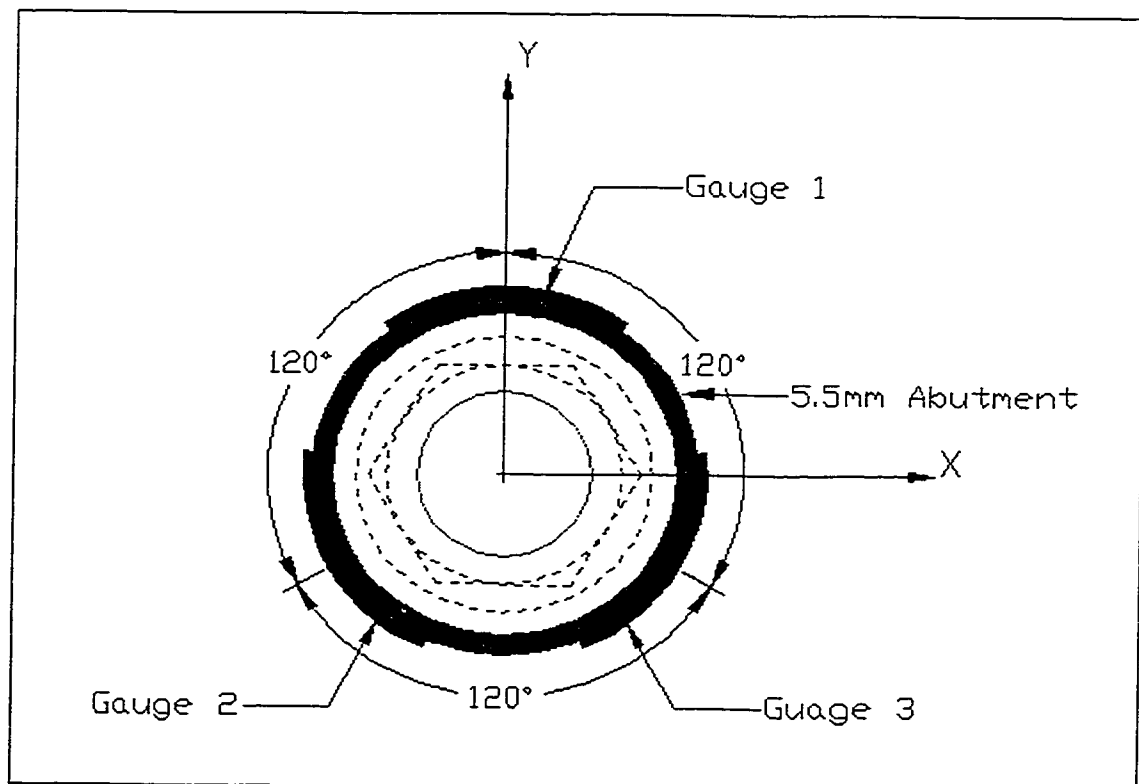**Figure B-1: Calibration Force and Bending Moment**

Figure B-2: Strain Gauge Orientation

Appendix C

Patient *In Vivo* Data

Study Information for Patients

Why is this study being done?

There is not much known about the stress and strain on an implant. This stress and strain is caused by **loading** of the implant, and we believe it is important to understand more about this **load**.

Bone is always replacing itself. Bones working hard and experiencing high stress need to replace themselves more than bones under less stress. Bones around the osseointegrated implants are thought to experience high stress. They need to be repairing the microscopic damage caused by the implants.

We are doing this study to learn more about the loading of an implant. If the load is too great and/or the bone is not healthy, the implant may not stay in. The information we gather will help us to plan the best care possible.

We will be studying two types of implant load. They are:

Preload – this load is always present and results from the bar superstructure being attached to the implant(s)

Functional Load – the loading that occurs with daily activities such as attaching or removing a prosthesis, chewing or talking.

What is being studied?

We will study:

1. The load delivered to the implant when your bar superstructure is tightened.

2. The load delivered when you put on and take off your prosthesis.

If you go into this study, what will take place?

Firstly, you will sign a consent form to say you agree to take part in the study.

A visit will then be set up for you at COMPRU. This visit will take approximately 4-5 hours.

During the visit the following will take place:

- your prosthesis and bar superstructure will be removed
- a Periotest® will be made on all the abutments
- your abutments will be replaced with study abutments
- the study abutments will be tested with a Periotest®

- the fit of your bar superstructure will be checked
- the gold screws that fasten the bar superstructure to the abutments will be tightened one at a time, and load measurements will be taken after each tightening
- you will then take off, then put on your prosthesis
- the study abutments will then be removed and your own put back on
- a Periotest® will be done again
- the fit of your prosthesis will be checked and then you are free to go

Removing and reattaching the abutments does not usually cause much discomfort. If discomfort occurs, we can apply a gel to the sight to numb the feeling.

Who can take part in this study?

You can take part in this study if you have an osseointegrated implant for auricular reconstruction (if you did not have a temporal bone resection as well) or orbital/facial reconstruction. The implant must be at least a year old.

You cannot take part in the study if you have:

- a pacemaker
- serious skin responses around the abutments
- problems with the stability of your implant
- any heart valve problems

What are the benefits and risks if you take part in this study?

Benefits:

There are no direct benefits to you, but by doing research we always look to learn more, and thus improve on the future care we provide to people with your kind of problem.

Risks:

We cannot tell before we start how well integrated an implant is. Each time an abutment is taken off or put back on there is the risk of disturbing an implant that is not well integrated. It is possible in such cases that integration may be lost. If loss of integration does occur, plans will be made for implant replacement, and you may not be able to wear the prosthesis until replacement is complete.

After abutment changing, some skin response may occur. This is usually mild. We will apply Sofracort ointment after the procedure. You will follow your usual hygiene habits. You can call COMPRU if you have a skin response that concerns you.

Can you leave the study?

You can leave the study at any time. This **will not** alter the care you are receiving now, or in the future.

Confidentiality:

The information from the study will be shared with people working and learning in this field. This will be done through lectures and writings in professional journals. Your name will not be used, but slides and pictures may reveal your identity.

Who you contact for more information about this study.

Should you need to contact anyone at anytime about the study, contact names and numbers are:

Dr. John Wolfaardt Director, COMPRU	Work	(780) 930-5660
Dr. Gordon Wilkes Director, COMPRU	Work	(780) 930-5660
Gail Hufty Business Leader, COMPRU	Work	(780) 930-5660

An In Vivo Evaluation of Stress Transfer to Craniofacial Implants

Consent Form

I certify that the written information outlining the general study considerations and potential problems and risks was presented to me. I have read the material and understand its contents. I also understand that potential problems and risks may include, but are not limited to, those described in the written material.

I have had the opportunity to discuss the information supplied to me to clarify any areas I did not understand.

I understand that I may withdraw from the study at any time.

I consent to participate in the study. I also give permission for the use of photographs/slides made in the course of the study to be used for the purposes of research, education and publication in professional journals and release any interest I have in these photographs/slides. I acknowledge that any such use is not an invasion of my privacy.

Signed:_____   _____ /_____ /1999

                               Name   Day   Month

Appendix D

Free Body Diagram

Contact force, C1, between gold screw and gold cylinder.

Preload, P, in gold screw.

Contact force, C1, between gold screw and gold cylinder.

Contact force, C2, between gold cylinder and abutment.

Contact force, P', between abutment and abutment screw.

Force, P, from gold screw.

Misfit load, M, between abutment screw and implant.

Contact force, C2, between gold cylinder and abutment.

Contact force, P', between abutment and abutment screw.

Contact force, M, between abutment and implant.

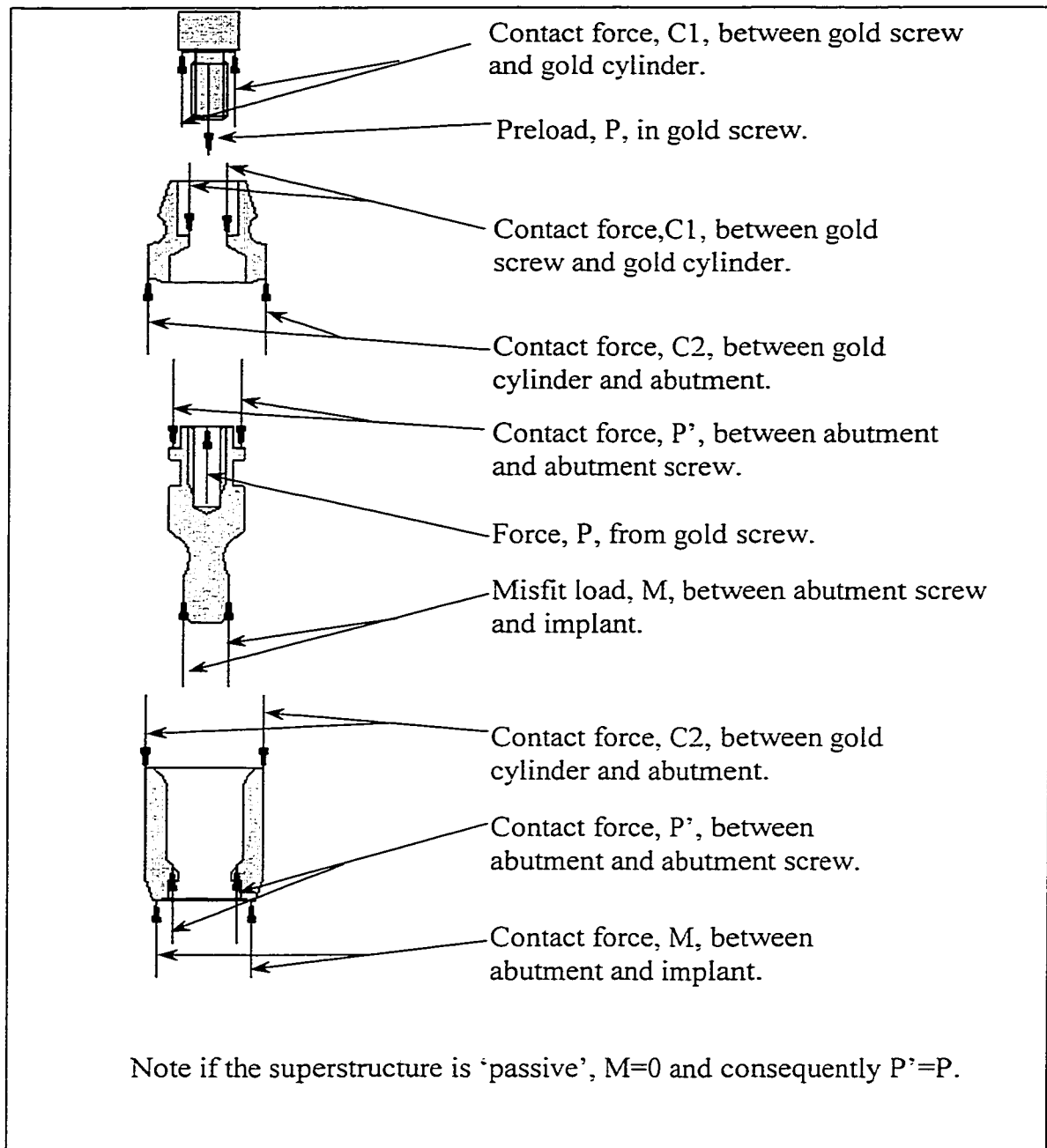Note if the superstructure is 'passive', M=0 and consequently P'=P.

Figure D-1: Free Body Diagram Components of an Auricular Retention System